Safe and Dynamically-Feasible Motion Planning using Control Lyapunov and Barrier Functions

Pol Mestres   Carlos Nieto-Granda   Jorge Cortés

Abstract—This paper considers the problem of designing motion planning algorithms for control-affine systems that generate collision-free paths from an initial to a final destination and can be executed using safe and dynamically-feasible controllers. We introduce the `C-CLF-CBF-RRT` algorithm, which produces paths with such properties and leverages rapidly exploring random trees (RRTs), control Lyapunov functions (CLFs) and control barrier functions (CBFs). We show that `C-CLF-CBF-RRT` is computationally efficient for a variety of different dynamics and obstacles, and establish its probabilistic completeness. We showcase the performance of `C-CLF-CBF-RRT` in different simulation and hardware experiments.

I. INTRODUCTION

Motion planning refers to the problem of computing a collision-free trajectory for a mobile agent to go from an initial state to a goal state. Motion planning algorithms are the backbone of many robotics applications, but their implementation remains challenging for robots with complex dynamics and environments with irregular obstacles. Even in scenarios where the robot dynamics and the environment obstacles are known, obtaining motion plans is in general a challenging task. Most motion planning algorithms generate high-level plans, consisting of sequences of waypoints in the configuration space, and assume the availability of low-level controllers that can follow such waypoints while avoiding collisions with obstacles. An example of low-level controllers frequently used in applications requiring collision-free navigation are those based on control barrier functions (CBFs) for safety and control Lyapunov functions (CLFs) for stability. However, controllers that simultaneously address safety and stability of the different waypoints might in general be not well-defined. This work is motivated by the need to bridge the gap between motion planner implementations and low-level CLF-CBF controllers that produce dynamically feasible safe trajectories.

Literature Review: Sampling-based motion planning [1] seeks to find a collision-free path from an initial state to a goal state through randomly sampling the state space. Despite its simplicity, it has been shown to be a practical solution for efficiently finding feasible paths even for high-dimensional problems. Rapidly-exploring random trees (RRTs) [2] and its variants [3], [4] are a family of sampling-based motion planning algorithms that are simple to implement and are probabilistically complete, meaning that a feasible path (if it exists) is found with probability one as the number of

P. Mestres and J. Cortés are with the Department of Mechanical and Aerospace Engineering, University of California, San Diego, {pomestre,cortes}@ucsd.edu. Carlos Nieto-Granda is with the DEV-COM US Army Research Laboratory (ARL), Adelphi, Maryland, carlos.p.nieto2.civ@army.mil.

samples goes to infinity. RRTs build a tree rooted at a starting configuration and efficiently explore the configuration space by adding more samples. Despite the widespread use of RRT and the variants outlined above, their performance in systems with general differential constraints and dynamics remains limited, since they rely on the ability to connect any neighboring nodes of the tree with a dynamically feasible trajectory. This requires solving a *two-point boundary value problem* (BVP) [5, Chapter 14], which in general is challenging. Different works [6], [7] address this problem by developing algorithms that achieve optimality guarantees for different classes of systems without requiring the use of a BVP solver. On the one hand, [6] considers controllable linear systems, for which the explicit solution of the BVP can be computed, and [7] focuses on non-holonomic systems where *Chow's condition* holds, whose accessibility properties can also be used to sidestep the use of a BVP solver. Alternatively, other works introduce heuristics that approximate the solution of the BVP: [8], [9] do it using the linear quadratic regulator, and [10] leverages bang-bang controllers. Other works circumvent solving the BVP by using learning-based approaches. For instance, [11], [12] introduces an offline machine learning phase that learns the solution of the BVP, [13] refines the generation of the dataset used in this offline phase, and [14] learns the solution of the BVP using reinforcement learning techniques.

Here we bypass the need to solve the BVP by using two sets of well-established tools: control Lyapunov functions (CLFs) [15], for designing stabilizing controllers for nonlinear systems, and control barrier functions (CBFs) [16], [17], for rendering safe a desired set. In applications where safety and stability specifications need to be met simultaneously, the CLF and CBF conditions can be combined in a variety of different formulations including a quadratic program with a relaxation variable [18], safety filters [19] (where the CBF condition acts on top of a stabilizing nominal controller), or designs based on penalty methods [20]. Even though these control designs have shown great success in applications such as adaptive cruise control [21] and bipedal walking [22], different works have shown that, when combined, they can lead to the existence of undesirable equilibria [23]–[25], which can even be asymptotically stable and have large regions of attraction, or the lack of feasibility [20], [26], [27] between the CBF and CLF conditions.

There exist a few works in the literature [28]–[31] that combine the effectiveness of RRT-based algorithms with the guarantees and computational efficiency provided by CBFs and CLFs, hence also bypassing the need to compute the solution of a BVP. However, these approaches require the simulation of trajectories derived from a CLF-CBF-based

controller in order to determine whether new candidate nodes should be added to the tree. The repeated simulation of such trajectories can significantly slow down the search for a feasible path and compromise the computational efficiency of the resulting algorithm. Moreover, these existing works do not formally ensure that the low-level CLF and CBF-based controller possesses both safety and stability guarantees.

Statement of Contributions: We consider the problem of designing motion planning algorithms that generate collison-free paths from an initial to a final destination for systems with control-affine dynamics. To ensure that the sequence of waypoints generated by the sampling-based algorithm can be tracked by a suitable controller while ensuring safety and stability, we leverage the theory of CBFs and CLFs. First, we introduce a result of independent interest which shows that the problem of verifying whether a CLF and a CBF are compatible in a set of interest can be solved by finding the optimal value of an optimization problem. We also show that for linear systems and polytopic CBFs, such optimization problem reduces to a quadratically constrained quadratic program (QCQP), and for circular CBFs it can be solved in closed form. Next, we leverage these results to develop a variant of RRT, which we call Compatible CLF-CBF-RRT (or `C-CLF-CBF-RRT` for short) that generates collision-free paths that can be executed with a CLF-CBF-based controller, and show that it is probabilistically complete. Compared to other approaches in the literature, our results on the compatibility verification of CBFs and CLFs can be leveraged to ensure that the computational complexity of `C-CLF-CBF-RRT` is tractable. Furthermore, we show how our proposed approach can be generalized to systems where safety constraints have a high relative degree. We illustrate our results in simulation and hardware experiments for differential drive robots and compare them with other approaches in the literature.

II. PRELIMINARIES

This section introduces the notation and preliminaries on control Lyapunov functions, control barrier functions, and rapidly exploring random trees.

A. Notation

We denote by $\mathbb{Z}_{>0}$, $\mathbb{R}$, and $\mathbb{R}_{\geq 0}$ the set of positive integers, real, and nonnegative real numbers, resp. For $N \in \mathbb{Z}_{>0}$, we denote $[N] = \{1, 2, \ldots, N\}$. Given $x \in \mathbb{R}^n$, $\|x\|$ denotes its Euclidean norm. Let $B \in \mathbb{R}^{n \times m}$ be a matrix. We denote by $\mathrm{Im}(B)$ its image. Given a set $\mathcal{S} \subset \mathbb{R}^n$, we denote its boundary by $\partial \mathcal{S}$ and its closure by $\mathrm{Cl}(\mathcal{S})$. We denote by $\mathcal{B}(x, \delta)$ the Euclidean closed ball of center $x \in \mathbb{R}^n$ and radius $\delta > 0$, i.e., $\mathcal{B}(x, \delta) := \{y \in \mathbb{R}^n : \|y - x\| \leq \delta\}$. Given an arbitrary set A, we refer by $\mathcal{P}(A)$ to the power set of A, i.e., the set of all subsets of A, including the empty set and A itself. The symbols $\mathbb{I}_n$, $\mathbb{0}_n$ denote the identity and zero matrices of dimension $n \in \mathbb{Z}_{>0}$, and $\mathbf{0}_n$ is the zero vector of dimension n. Given $f : \mathbb{R}^n \to \mathbb{R}^n$, $g : \mathbb{R}^n \to \mathbb{R}^{n \times m}$ and a smooth $W : \mathbb{R}^n \to \mathbb{R}$, the notation $L_f W : \mathbb{R}^n \to \mathbb{R}$ (resp., $L_g W : \mathbb{R}^n \to \mathbb{R}^m$) denotes the Lie derivative of W with respect to f (resp., g), that is $L_f W = \nabla W^T f$ (resp., $\nabla W^T g$). A function $\beta : \mathbb{R} \to \mathbb{R}$ is extended class $\mathcal{K}_\infty$ if it is continuous, $\beta(0) = 0$, β is strictly increasing and $\lim_{s \to \pm\infty} \beta(s) = \pm\infty$. A function $V : \mathbb{R}^n \to \mathbb{R}$ is positive definite with respect to $q \in \mathbb{R}^n$ if $V(q) = 0$ and $V(x) > 0$ for $x \neq q$. Given a locally Lipschitz function $f : \mathbb{R}^n \to \mathbb{R}$, its generalized gradient at $x \in \mathbb{R}^n$ is $\partial f(x) = \mathrm{co}\{\lim_{i \to \infty} \nabla f(x_i) : x_i \to x, x_i \notin S \cup \Gamma_f\}$, where Γ_f is the zero-measure set where f is non-differentiable and S is any set of measure zero. An undirected graph $\mathcal{M}$ is a pair $\mathcal{M} = (V, \mathcal{E})$, where $V = \{1, \ldots, N\}$ is a finite set called the vertex set, $\mathcal{E} \subset V \times V$ is called the edge set where $(i, j) \in \mathcal{E}$ if and only if $(j, i) \in \mathcal{E}$. A path in $\mathcal{M}$ is a sequence of vertices $v_1, \ldots, v_k$, with $k \in \mathbb{Z}_{>0}$, such that for all $i \in [k-1]$, $(v_i, v_{i+1}) \in \mathcal{E}$. A tree is an undirected graph in which there exists a single path between any pair of vertices.

B. Control Lyapunov Functions and Nonsmooth Control Barrier Functions

This section presents preliminaries on control Lyapunov functions. Consider a control-affine system

$$\dot{x} = f(x) + g(x)u, \tag{1}$$

where $f : \mathbb{R}^n \to \mathbb{R}^n$ and $g : \mathbb{R}^n \to \mathbb{R}^{n \times m}$ are locally Lipschitz functions, with $x \in \mathbb{R}^n$ the state and $u \in \mathbb{R}^m$ the input. Throughout the paper, and without loss of generality, we assume $f(0) = 0$, so that the origin $x = 0$ is the desired equilibrium point of the (unforced) system.

We start by recalling the notion of Control Lyapunov function (CLF) [32], [33].

Definition II.1. *(Control Lyapunov Function): Given an open set $\mathcal{D} \subseteq \mathbb{R}^n$, a point $q \in \mathbb{R}^n$ with $q \in \mathcal{D}$, a continuously differentiable function $V : \mathbb{R}^n \to \mathbb{R}$ is a **CLF** with respect to q in $\mathcal{D}$ for the system* (1) *if*

- *V is proper in $\mathcal{D}$, i.e., $\{x \in \mathcal{D} : V(x) \leq c\}$ is a compact set for all $c > 0$,*
- *V is positive definite with respect to q,*
- *there exists a continuous positive definite function $W : \mathbb{R}^n \to \mathbb{R}$ with respect to q such that, for each $x \in \mathcal{D}$, there exists a control $u \in \mathbb{R}^m$ satisfying*

$$L_f V(x) + L_g V(x)u \leq -W(x). \tag{2}$$

CLFs provide a way to guarantee asymptotic stability of the origin. Namely, if a Lipschitz controller $u_{\text{st}} : \mathbb{R}^n \to \mathbb{R}^m$ is such that, for every $x \in \mathcal{D}$, $u = u_{\text{st}}(x)$ satisfies (2), then the origin is asymptotically stable for the closed-loop system [32]. Such controllers can be synthesized by means of the pointwise minimum-norm (PMN) control optimization [33, Chapter 4.2],

$$u(x) = \arg \min_{u \in \mathbb{R}^m} \frac{1}{2} \|u\|^2$$
$$\text{s.t. (2) holds.}$$

Note that, at each $x \in \mathbb{R}^n$, this is a quadratic program in u.

Next we define the notion of Boolean Nonsmooth Control Barrier Function (BNCBF), adapted from [34, Definition II.8].

Definition II.2. *(BNCBF [34, Definition II.8]): Given $N \in \mathbb{Z}_{>0}$, let $h_i : \mathbb{R}^n \to \mathbb{R}$, for $i \in [N]$, be continuously differentiable functions. Let $h(x) = \max_{i \in [N]} h_i(x)$ and*

$$\mathcal{C} = \{x \in \mathbb{R}^n : h(x) \geq 0\}, \tag{3a}$$

$$\partial \mathcal{C} = \{x \in \mathbb{R}^n \ : \ h(x) = 0\}. \tag{3b}$$

Suppose that the set $\mathcal{C}$ is nonempty. Then, h is a BNCBF of $\mathcal{C}$ for (1) if there exists a locally Lipschitz extended class $\mathcal{K}_\infty$ function $\alpha : \mathbb{R} \to \mathbb{R}$ such that for every $x \in \mathcal{C}$ there exists $u \in \mathbb{R}^m$ such that,

$$\min_{v \in \partial h(x)} v^T(f(x) + g(x)u) \geq -\alpha(h(x)).$$

In case $N = 1$, Definition II.2 reduces to the standard notion of Control Barrier Function [16, Definition 2]. Given $x \in \mathbb{R}^n$, let $\mathcal{I}(x) := \{i \in [N] \ : \ h(x) = h_i(x)\}$ denote the set of *active* functions. The following result is adapted from [34, Theorem III.6] and provides a sufficient condition for h to be a BNCBF.

Proposition II.3. *(Sufficient Condition for BNCBF): Suppose there is an extended class $\mathcal{K}_\infty$ function $\alpha : \mathbb{R} \to \mathbb{R}$ such that, for all $x \in \mathbb{R}^n$, there exists $u \in \mathbb{R}^m$ with*

$$L_f h_i(x) + L_g h_i(x)u \geq -\alpha(h(x)), \tag{4}$$

for all $i \in \mathcal{I}(x)$. Then, h is a BNCBF of $\mathcal{C}$.

If a measurable and locally bounded controller $u_{\text{sf}} : \mathbb{R}^n \to \mathbb{R}^m$ is such that, for every $x \in \mathbb{R}^n$, $u = u_{\text{sf}}(x)$ satisfies (4), then u_{sf} renders $\mathcal{C}$ forward invariant (cf. [34, Theorem II.7, Definition II.8]).

When dealing with both safety and stability specifications, it is important to note that an input u might satisfy (2) but not (4), or vice versa. The following notion, adapted from [27, Definition 2.3], captures when a CLF V and a BNCBF h are compatible.

Definition II.4. *(Compatibility of CLF-BNCBF pair): Let $\mathcal{D} \subseteq \mathbb{R}^n$ be open, $\mathcal{C} \subset \mathcal{D}$ be closed, V a CLF on $\mathcal{D}$ and h a BNCBF of $\mathcal{C}$. Then, V and h are compatible in a set $\tilde{\mathcal{D}} \subset \mathcal{D}$ if there exist a positive definite function $W : \mathbb{R}^n \to \mathbb{R}$ and an extended class $\mathcal{K}_\infty$ function $\alpha : \mathbb{R} \to \mathbb{R}$ such that, for all $x \in \tilde{\mathcal{D}}$, there exists $u \in \mathbb{R}^m$ satisfying (2) and (4) for all $i \in \mathcal{I}(x)$ simultaneously.*

If V and h are compatible in a set $\tilde{\mathcal{D}}$, we can define the minimum norm controller that satisfies the CLF and BNCBF conditions $u^* : \tilde{\mathcal{D}} \to \mathbb{R}^m$ as follows:

$$u^*(x) := \arg \min_{u \in \mathbb{R}^m} \frac{1}{2} \|u\|^2 \tag{5}$$
$$\text{s.t. } L_f V(x) + L_g V(x)u \leq -W(x),$$
$$L_f h_i(x) + L_g h_i(x)u \geq -\alpha(h(x)), \ \forall \ i \in \mathcal{I}(x).$$

If u^* is locally Lipschitz, then it ensures that $\mathcal{C}$ is forward invariant and that the origin is asymptotically stable for the closed-loop system.

C. Rapidly-exploring Random Trees (RRTs)

Here, we review GEOM-RRT [3], cf. Algorithm 1, a version of RRT [2] upon which we rely later. The input for GEOM-RRT consists of a state space $\mathcal{X}$, an initial configuration x_{init}, goal region $\mathcal{X}_{\text{goal}}$, number of iterations k, and a steering parameter η whose use is defined in the sequel. The algorithm builds a tree $\mathcal{T}$ by executing k iterations of the following form:

> At each iteration, a new random sample x_{rand} is obtained by uniformly sampling $\mathcal{X}$

Algorithm 1 GEOM-RRT

1: **Parameters**: $x_{\text{init}}, \mathcal{X}_{\text{goal}}, k, \eta$
2: $\mathcal{T}.\text{init}(x_{\text{init}})$
3: **for** $i \in [1, \ldots, k]$ **do**
4:     $x_{\text{rand}} \leftarrow$ RANDOM_STATE
5:     $x_{\text{near}} \leftarrow$ NEAREST_NEIGHBOR$(x_{\text{rand}}, \mathcal{T})$
6:     $x_{\text{new}} \leftarrow$ NEW_STATE$(x_{\text{rand}}, x_{\text{near}}, \eta)$
7:     **if** COLLISION_FREE$(x_{\text{near}}, x_{\text{new}})$ **then**
8:         $\mathcal{T}.\text{add\_vertex}(x_{\text{new}})$
9:         $\mathcal{T}.\text{add\_edge}(x_{\text{near}}, x_{\text{new}})$
10:         **if** $x_{\text{new}} \in \mathcal{X}_{\text{goal}}$ **then**
11:             **return** $\mathcal{T}$
12:         **end if**
13:     **end if**
14: **end for**
15: **return** $\mathcal{T}$

---

using RANDOM_STATE(). The function NEAREST_NEIGHBOR$(x_{\text{rand}}, \mathcal{T})$ returns the vertex x_{near} from $\mathcal{T}$ that is closest in the Euclidean distance to x_{rand}. Next, a new configuration $x_{\text{new}} \in \mathcal{X}$ is returned by the NEW_STATE function such that x_{new} is on the line segment between x_{near} and x_{rand} and the distance $\|x_{\text{near}} - x_{\text{new}}\|$ is at most η. Finally, the function COLLISION_FREE$(x_{\text{near}}, x_{\text{new}})$ checks whether the straight line from x_{near} and x_{new} is collision free. If this is the case, x_{new} is added as a vertex to $\mathcal{T}$ and is connected by an edge from x_{near}. If $x_{\text{new}} \in \mathcal{X}_{\text{goal}}$, there exists a single path in $\mathcal{T}$ from x_{init} to x_{new}.

A notable property of GEOM-RRT is that it is *probabilistically complete*, meaning that the probability that the algorithm will return a collision-free path from the initial state to the goal state (if one exists) approaches one as the number of iterations tends to infinity [35].

III. PROBLEM STATEMENT

Let $\mathcal{R}$ be a compact and convex set in $\mathbb{R}^n$ containing M known obstacles $\{\mathcal{O}_l\}_{l=1}^M$, with $\text{Int}(\mathcal{O}_i) \cap \text{Int}(\mathcal{O}_j) = \emptyset$ for all $i \neq j \in [M]$. Let $\mathcal{F} := \mathcal{R} \setminus \cup_{l=1}^M \mathcal{O}_l$ denote the *safe space*. For each $l \in [M]$, we assume that there exists a positive integer $N_l \in \mathbb{Z}_{>0}$ and known continuously differentiable functions $\{h_{i,l} : \mathbb{R}^n \to \mathbb{R}\}_{i \in [N_l]}$ such that $\mathcal{O}_l := \{x \in \mathbb{R}^n \ : \ h_l(x) = \max_{i \in [N_l]} h_{i,l}(x) < 0\}$. Even though this imposes a specific structure on the set $\mathcal{O}_l$, one can obtain more complex obstacles by considering sets of the form $\cup_{i \in \mathcal{M}} \mathcal{O}_i$, with $\mathcal{M}$ a subset of $[M]$.

The robot dynamics are control-affine of the form (1), with $f : \mathbb{R}^n \to \mathbb{R}^n$ and $g : \mathbb{R}^n \to \mathbb{R}^m$ locally Lipschitz. For each $l \in [M]$, h_l is a BNCBF of $\mathbb{R}^n \setminus \mathcal{O}_l$ for these dynamics, with associated extended class $\mathcal{K}_\infty$ function α_l. We also assume that

$$\nabla h_{i,l}(x)^T g(x) \neq \mathbf{0}_m, \quad \forall x \in \mathcal{F}, l \in [M], i \in [N_l],$$

i.e., one differentiation of $h_{i,l}$ already makes the input u appear explicitly. We let $\mathcal{I}_l(x) = \{i \in [N_l] \ : \ h_l(x) = h_{i,l}(x)\}$. Given an initial state $x_{\text{init}} \in \mathcal{R}$ and a final goal set $\mathcal{X}_{\text{goal}} \subset \mathcal{R}$,

our aim is to develop a sampling-based motion planning algorithm that constructs a collision-free path $\mathcal{A} := \{x_i\}_{i=1}^{N_a}$ from x_{init} to $\mathcal{X}_{\text{goal}}$ that is dynamically feasible, i.e., such that for each pair of consecutive waypoints in $\mathcal{A}$, there exists a control law that generates a safe trajectory that connects them. Our approach to solve this problem leverages the theory of CLFs and BNCBFs to design controllers which (i) have safety and stability guarantees by design, and (ii) can be implemented efficiently to help reduce the computational burden of generating dynamically feasible trajectories.

IV. CLF AND BNCBF COMPATIBILITY VERIFICATION

The key challenge in our proposed approach to the problem outlined in Section III is that the optimization (5) defining the CLF-CBF-based controller has to be feasible at all points along the trajectory. In this section we tackle this problem and show how such a feasibility check can be performed in general, and how it is efficient in two specific cases of interest.

A. Compatibility Verification for General Dynamics and Obstacles

In this section we consider the problem of verifying that a CLF and a BNCBF are compatible in systems for general dynamics and obstacles. The following result gives a characterization for when a CLF and a BNCBF are compatible in the region $\mathcal{R}$.

Proposition IV.1. *(Characterization of CLF-BNCBF Compatibility):* Given $q \in \mathcal{F}$, let $V_q : \mathbb{R}^n \to \mathbb{R}$ be a CLF of (1) with respect to q. Let $l \in [M]$ and assume that h_l is a BNCBF of $\mathbb{R}^n \backslash \mathcal{O}_l$. Let $W_q : \mathbb{R}^n \to \mathbb{R}$ be a positive definite function with respect to q and $\alpha_l : \mathbb{R} \to \mathbb{R}$ be an extended class $\mathcal{K}_\infty$ function. For each $\mathcal{J} \subset \mathcal{P}([N_l])$, let $Z_{l,\mathcal{J}} := \{x \in \mathbb{R}^n : \mathcal{I}_l(x) = \mathcal{J}\}$ denote the set of points where the active constraints defining obstacle $\mathcal{O}_l$ correspond to the indices in $\mathcal{J}$. For $\Gamma \subset \mathcal{R}$, define

$$\zeta_1 = \min_{\substack{x \in \Gamma \\ \{\beta_i \in \mathbb{R}\}_{i \in \mathcal{J}}}} \left\| \sum_{i \in \mathcal{J}} \beta_i L_g h_{i,l}(x) - L_g V_q(x) \right\|^2 \quad (6a)$$

$$\text{s.t.} \quad \beta_i \geq 0, \ i \in \mathcal{J}, \quad (6b)$$

$$h_{j,l}(x) \leq h_{i,l}(x), \ \forall j \notin \mathcal{J}, i \in \mathcal{J}, \quad (6c)$$

$$h_l(x) \geq 0. \quad (6d)$$

If $\zeta_1 \neq 0$, then V_q and h_l are compatible in $Z_{l,\mathcal{J}} \cap \Gamma \cap \mathcal{F}$. Otherwise, if $\zeta_1 = 0$, let

$$\zeta_2 = \min_{\substack{x \in \Gamma \\ \{\beta_i \in \mathbb{R}\}_{i \in \mathcal{J}}}} \Phi(x, \{\beta_i\}_{i \in \mathcal{J}}), \quad (7a)$$

$$\text{s.t.} \quad \sum_{i \in \mathcal{J}} \beta_i L_g h_{i,l}(x) = L_g V_q(x), \quad (7b)$$

$$\beta_i \geq 0, \ i \in \mathcal{J}, \quad (7c)$$

$$h_{j,l}(x) \leq h_{i,l}(x), \ \forall j \notin \mathcal{J}, i \in \mathcal{J}, \quad (7d)$$

$$h_l(x) \geq 0, \quad (7e)$$

for $\Phi(x, \{\beta_i\}_{i \in \mathcal{J}}) = -W_q(x) - L_f V_q(x) + \sum_{i \in \mathcal{J}} \beta_i(L_f h_{i,l}(x) + \alpha_l(h_{i,l}(x)))$. *If $\zeta_2 \geq 0$, then V_q and h_l are compatible in $Z_{l,\mathcal{J}} \cap \Gamma \cap \mathcal{F}$. Conversely, if V_q and h_l are compatible in $Z_{l,\mathcal{J}} \cap \Gamma \cap \mathcal{F}$ then there exists*

an extended class $\mathcal{K}_\infty$ function α_l and a positive definite function W_q with respect to q such that either $\zeta_1 \neq 0$ or $\zeta_1 = 0$ and $\zeta_2 \geq 0$.

Proof. First note that if $\zeta_1 = 0$, the optimization problem (7) is feasible and therefore ζ_2 is well-defined. By Farkas' Lemma [36], V_q and h_l are compatible at $x \in Z_{l,\mathcal{J}} \cap \Gamma \cap \mathcal{F}$ if and only if for some positive definite function with respect to q W_q and some extended class $\mathcal{K}_\infty$ function α_l, there do not exist $\beta_0 \in \mathbb{R}_{\geq 0}$, $\{\beta_i\}_{i \in \mathcal{J}} \subset \mathbb{R}_{\geq 0}$ such that

$$\beta_0 L_g V_q(x) = \sum_{i \in \mathcal{J}} \beta_i L_g h_{i,l}(x), \quad (8a)$$

$$\beta_0(-L_f V_q(x) - W(x))$$
$$+ \sum_{i \in \mathcal{J}} \beta_i(\alpha_l(h_{i,l}(x)) + L_f h_{i,l}(x)) < 0. \quad (8b)$$

First suppose that for some W_q and α_l, either $\zeta_1 \neq 0$ or $\zeta_1 = 0$ and $\zeta_2 \geq 0$. Suppose there exists a solution $s_1^* = (x^*, \beta_0^*, \{\beta_i^*\}_{i \in \mathcal{I}_l(x)})$ of (8) and let us reach a contradiction. If $\beta_0^* = 0$, then, (8) implies that the constraints $L_f h_{i,l}(x) + L_g h_{i,l}(x)u \geq -\alpha_l(h_{i,l}(x))$ are not simultaneously feasible, which means that h_l is not a BNCBF, hence arriving at a contradiction. Therefore, s_1^* must be such that $\beta_0^* > 0$. By taking $\tilde{\beta}_i = \frac{\beta_i}{\beta_0}$ for $i \in \mathcal{J}$, we deduce that $(x^*, \{\tilde{\beta}_i\}_{i \in \mathcal{J}})$ is a solution of (6) with a value of the objective function equal to zero. This means that if $\zeta_1 \neq 0$, the solution s_1^* does not exist and V_q and h_l are compatible in $Z_{l,\mathcal{J}} \cap \Gamma \cap \mathcal{F}$. Otherwise, if $\zeta_1 = 0$, then $(x^*, \{\tilde{\beta}_i\}_{i \in \mathcal{J}})$ is a solution of (7) with a strictly negative value of the objective function. This means that if $\zeta_1 = 0$ and $\zeta_2 \geq 0$, the solution s_1^* does not exist and V_q and h_l are compatible in $Z_{l,\mathcal{J}} \cap \Gamma \cap \mathcal{F}$. Conversely, suppose that V_q and h_l are compatible in $Z_{l,\mathcal{J}} \cap \Gamma \cap \mathcal{F}$. This implies that there exists W_q and α_l such that (8) has no solution. If (8a) has no solution, then $\zeta_1 \neq 0$. If (8a) has a solution but (8b) does not, then $\zeta_1 = 0$ and $\zeta_2 \geq 0$. $\square$

Note that Proposition IV.1 is valid for any set $\Gamma \subset \mathcal{R}$. Often, one is interested in verifying the compatibility of a CLF and a BNCBF only in a small subset of $\mathcal{R}$, in which case the flexibility provided by the set Γ is useful.

Remark IV.2. *(Checking for all Possible Sets of Active Constraints):* Given a subset $\mathcal{J} \subset \mathcal{P}([N_l])$ of functions $\{h_{i,l}\}$, Proposition IV.1 provides a way to verify if the CLF and the BNCBF are compatible at the points in the region of interest $\Gamma \cap \mathcal{F}$ where such functions are active. Let $H_{l,\mathcal{J}} := \{x \in \Gamma : \mathcal{I}_l(x) = \mathcal{J}\}$ be the points in Γ where the constraints with index in $\mathcal{J}$ are active, and $\mathcal{S}_l := \{\mathcal{J} \subset \mathcal{P}([N_l]) : H_{l,\mathcal{J}} \neq \emptyset\}$ be the sets of indices for which the above set is nonempty. The class $\mathcal{S}_l$ contains all possible sets of active constraints in Γ. By checking the condition in Proposition IV.1 for all $\mathcal{J}$ in $\mathcal{S}_l$, we can verify if the CLF and the BNCBF are compatible in $\Gamma \cap \mathcal{F}$. In practice, given a region Γ where we are interested in checking the compatibility of V_q and h_l, one can often identify the indices that can achieve a maximum value in Γ (for example, for polytopic obstacles in the plane, only a few of the functions $h_{i,l}$ have points in Γ where they take positive values). This means that the cardinality of $\mathcal{S}_l$ is often small and the number of checks using Proposition IV.1 can be kept small. ●

Remark IV.3. *(Verifying Compatibility for Multiple BNCBFs):* Proposition IV.1 actually provides a way to check whether the optimization problem (5) is feasible at *all* points of Γ. This can be done as follows: one first finds all $l \in [M]$ such that $\Gamma \cap \mathcal{O}_l \neq \emptyset$. If Γ can be expressed as the 0-sublevel set of a convex differentiable function γ, i.e., $\Gamma := \{x \in \mathbb{R}^n : \gamma(x) \leq 0\}$, and the functions $h_{i,l}$ are convex, then this can be solved efficiently by checking that the solution of the convex problem

$$\min_{x \in \mathbb{R}^n} \gamma(x)$$
$$\text{s.t. } h_{i,l}(x) \leq 0, \quad \forall i \in [N_l]$$

is non-positive. The BNCBF constraints associated with those $l' \in [M]$ such that $\Gamma \cap \mathcal{O}_{l'} = \emptyset$ can be neglected since, given a controller that satisfies all the other BNCBF constraints, it can be shown to also satisfy the BNCBF constraints for such $l' \in [M]$ by taking the corresponding extended class $\mathcal{K}_\infty$ function $\alpha_{l'}$ linear with sufficiently large slope. On the other hand, for $l' \in [M]$ such that $\Gamma \cap \mathcal{O}_{l'} \neq \emptyset$, Proposition IV.1 ensures that there exists a small neighborhood around $\partial \mathcal{O}_{l'}$, not containing points of any other obstacle, where V and $h_{l'}$ are compatible. By taking the extended class $\mathcal{K}_\infty$ functions of the other CBF constraints as linear functions with sufficiently large slope, (5) is feasible in each of these neighborhoods. Finally, for points in Γ not belonging to any of these neighborhoods, the extended class $\mathcal{K}_\infty$ functions can also be taken as linear with sufficiently large slope to guarantee that (5) is feasible. ●

Remark IV.4. *(About the Choice of CLF and Class $\mathcal{K}_\infty$ Function):* Note that, when solving the optimization problems (6) and (7) for fixed V_q, α_l, and W_q, it is not guaranteed that $\zeta_1 \neq 0$ or $\zeta_1 = 0$ and $\zeta_2 \geq 0$. If $\tilde{\alpha}$ is an extended class $\mathcal{K}_\infty$ function with $\tilde{\alpha}(s) \geq \alpha(s)$ for all $s \in \mathbb{R}$, the objective function Φ of (7) does not decrease at any point, which means that the value of ζ_1 remains the same, but the condition $\zeta_2 \geq 0$ becomes easier to satisfy. A similar behavior occurs if $\tilde{W}$ is a positive definite function with $\tilde{W}(x) \leq W(x)$ for all $x \in \mathbb{R}^n$. We leverage these observations in Section V when we introduce our proposed motion planning algorithm. ●

Remark IV.5. *(Regularity Properties of the Controller):* If V_q and h_l are compatible in $\mathcal{R}$ for all $l \in [M]$, the CLF-CBF-based controller (5) is well defined, i.e., the optimization (5) is feasible for all points in $\mathcal{R}$. However, slightly stronger conditions are needed to ensure that such CLF-CBF-based controller is locally Lipschitz and therefore can be used to render $\mathcal{C}$ forward invariant and the origin asymptotically stable. We refer the reader to [37] for a survey on different conditions that ensure continuity, Lipschitzness, and other regularity properties of optimization-based controllers of the form (5). These conditions are often satisfied in practice and are mostly related to the dynamics and the specific obstacles, which in our problem here are given and not subject to design. Therefore, throughout this work, we assume that (5) satisfies at least one of the sufficient conditions outlined in [37] that ensure that the resulting controller is locally Lipschitz. ●

Proposition IV.1 shows that the problem of checking whether a CLF and a BNCBF are compatible in a region of interest can be reduced to solving a pair of optimization problems. However, in general, the optimization problems (6) and (7) are not convex and can be computationally intractable. Our forthcoming exposition provides two particular cases of dynamics and obstacles for which these two optimization problems are computationally tractable.

B. Compatibility Verification for Linear Systems and Polytopic Obstacles

In this section we particularize our discussion to linear dynamics,

$$\dot{x} = Ax + Bu, \tag{9}$$

where $A \in \mathbb{R}^{n \times n}$, $B \in \mathbb{R}^{n \times m}$, and the obstacles are polytopic (i.e., the functions $h_{i,l}$ are affine). We start by introducing some useful notation. For each $l \in [M]$, let $a_{i,l} \in \mathbb{R}^n$, $b_{i,l} \in \mathbb{R}$ be such that $h_{i,l}(x) = a_{i,l}^T x + b_{i,l}$. We further assume that h_l is a BNCBF, i.e., there exists an extended class $\mathcal{K}_\infty$ function α_l such that, for all $x \in \mathbb{R}^n \backslash \mathcal{O}_l$, there exists $u \in \mathbb{R}^m$ with

$$a_{i,l}^T(Ax + Bu) \geq -\alpha_l(a_{i,l}^T x + b_{i,l})$$

for all $i \in \mathcal{I}_l(x)$. We further assume that given $q \in \mathbb{R}^n$, a quadratic CLF is available, i.e., we have a positive definite matrix $P \in \mathbb{R}^{n \times n}$ such that $V_q : \mathbb{R}^n \to \mathbb{R}$, defined as $V_q(x) = (x - q)^T P(x - q)$, is a CLF with respect to q in $\mathbb{R}^n$ of (9) with associated positive definite function $W_q : \mathbb{R}^n \to \mathbb{R}$.

The following result follows by applying Proposition IV.1 to the case when dynamics are linear and obstacles polytopic.

Proposition IV.6. *(Sufficient Condition for CLF-BNCBF Compatibility for Linear Dynamics and Polytopic Obstacles):* Let $\Gamma \subset \mathcal{R}$, $l \in [M]$, $\mathcal{J} \in \mathcal{P}([N_l])$, $q \in \mathcal{F}$, and define

$$\zeta_1 := \min_{\substack{x \in \Gamma \\ \{\beta_i \in \mathbb{R}\}_{i \in \mathcal{J}}}} \left\| \sum_{i \in \mathcal{J}} \beta_i B^T a_{i,l} - B^T P(x - q) \right\|^2 \tag{10a}$$

$$\text{s.t. } \beta_i \geq 0, \ \forall i \in \mathcal{J}, \tag{10b}$$
$$a_{j,l}^T x + b_{j,l} \leq a_{i,l}^T x + b_{i,l}, \ \forall j \notin \mathcal{J}, i \in \mathcal{J}, \tag{10c}$$
$$a_{i,l}^T x + b_{i,l} \geq 0, \ i \in \mathcal{J}. \tag{10d}$$

If $\zeta_1 \neq 0$, then V_q and h_l are compatible in $Z_{l,\mathcal{J}} \cap \Gamma \cap \mathcal{F}$. Otherwise, if $\zeta_1 = 0$, let

$$\zeta_2 := \min_{\substack{x \in \Gamma \\ \{\beta_i \in \mathbb{R}\}_{i \in \mathcal{J}}}} \Phi(x, \{\beta_i\}_{i \in \mathcal{J}}) \tag{11a}$$

$$\text{s.t. } \sum_{i \in \mathcal{J}} \beta_i B^T a_{i,l} = B^T P(x - q), \tag{11b}$$
$$\beta_i \geq 0, \ \forall i \in \mathcal{J}, \tag{11c}$$
$$a_{j,l}^T x + b_{j,l} \leq a_{i,l}^T x + b_{i,l}, \ \forall j \notin \mathcal{J}, i \in \mathcal{J}, \tag{11d}$$
$$a_{i,l}^T x + b_{i,l} \geq 0, \ i \in \mathcal{J}, \tag{11e}$$

with $\Phi(x, \{\beta_i\}_{i \in \mathcal{J}}) = -W_q(x) - (x - q)^T PAx + \sum_{i \in \mathcal{J}} \beta_i(\alpha_l(a_{i,l}^T x + b_{i,l}) + a_{i,l}^T Ax)$. *If* $\zeta_2 \geq 0$, then V_q and h_l are compatible in $Z_{l,\mathcal{J}} \cap \Gamma \cap \mathcal{F}$. Conversely, if V_q and h_l are compatible in $Z_{l,\mathcal{J}} \cap \Gamma \cap \mathcal{F}$, then there exists an extended class $\mathcal{K}_\infty$ function α_l and a positive definite function W_q with respect to q such that either $\zeta_1 \neq 0$ or $\zeta_1 = 0$ and $\zeta_2 \geq 0$.

We end this section by discussing the tractability of the optimizations (10) and (11). If W_q is a quadratic function (as

it is often the case in practice), $\alpha(s) = \alpha_0 s$, with $\alpha_0 > 0$, and Γ is given by a sublevel set of a quadratic function (e.g., if it is the sublevel set a quadratic CLF V_q), then (10) and (11) both have quadratic objective functions and quadratic constraints, i.e., they are quadratically constrained quadratic programs (QCQPs), for which efficient heuristics are available, see e.g. [38]. Note, however, that the quadratic objective functions might not be convex in the optimization variables, and therefore (10) and (11) might not be convex in general.

C. Compatibility Verification for Single Integrator and Circular Obstacles

In this section we consider single-integrator dynamics, i.e.,

$$\dot{x} = u, \tag{12}$$

and circular obstacles, i.e., $\mathcal{O}_l = \{x \in \mathbb{R}^n : \|x - c_l\| < r_l^2\}$ for some $c_l \in \mathbb{R}^n$ and $r_l > 0$. In this case, we take $h_l(x) = \|x - c_l\|^2 - r_l^2$, which is continuously differentiable and therefore $N_l = 1$ for all $l \in [M]$. We also take $V_q(x) = \|x - q\|^2$, and $W_q(x) = (x - q)^T Q(x - q)$, where $Q \in \mathbb{R}^{n \times n}$ is a positive definite matrix. Proposition IV.1 then takes the following form.

Proposition IV.7. *(Sufficient Condition for CLF-BNCBF Compatibility for Single Integrator Dynamics and Circular Obstacles): Let $l \in [M]$, $\alpha_l > 0$, $x_0 \in \mathbb{R}^n \backslash \{q\}$, $q \in \mathcal{F}$, $\Gamma := \{x \in \mathbb{R}^n : V_q(x) \le V_q(x_0)\}$, $B_l := \|q - c_l\|_Q^2 - 2\alpha_l r_l^2$,*

$$\beta_+ := \frac{\sqrt{B_l^2 + 4\alpha_l^2 r_l^2(\|q - c_l\|^2 - r_l^2)} - B_l}{2\alpha_l r_l^2},$$

and suppose that one of the following holds:

- $\|x_0 - q\| - \|c_l - q\| > 0$ *and* $\frac{\|x_0 - q\|}{\|x_0 - q\| - \|c_l - q\|} > 1 + \frac{\|c_l - q\|}{r_l}$;
- $\|x_0 - q\| - \|c_l - q\| > 0$, $\frac{\|x_0 - q\|}{\|x_0 - q\| - \|c_l - q\|} \le 1 + \frac{\|c_l - q\|}{r_l}$ *and* $\beta_+ \ge 1 + \frac{\|c_l - q\|}{r_l}$;
- $\|x_0 - q\| - \|c_l - q\| \le 0$.

Then, V_q and h_l are compatible in $\Gamma \cap \mathcal{F}$.

Proof. We rely on Proposition IV.1. In the setting considered here, (6) reads as

$$\zeta_1 := \min_{x \in \Gamma, \beta \in \mathbb{R}} \|2\beta(x - c_l) - 2(x - q)\|^2 \tag{13a}$$

$$\text{s.t. } \beta \ge 0, \tag{13b}$$

$$\|x - c_l\|^2 - r_l^2 \ge 0. \tag{13c}$$

It follows that $\zeta_1 = 0$ if and only if there exists $x \in \Gamma$ and $\beta \in \mathbb{R} \backslash \{1\}$ (note that $\beta = 1$ and $\zeta_1 = 0$ are not possible because $q \in \mathcal{F}$) such that $x = \frac{1}{\beta - 1}(\beta c_l - q)$, $\beta \ge 0$ and $\|x - c_l\|^2 - r_l^2 \ge 0$. Equivalently, $\zeta_1 = 0$ if and only if there exists $\beta \in \mathbb{R} \backslash \{1\}$ such that $\beta \ge 0$, $|\beta - 1| \le \frac{\|c_l - q\|}{r_l}$ and $\beta(\|x_0 - q\| - \|c_l - q\|) \ge \|x_0 - q\|$. Note that since $q \in \mathcal{F}$, $\|c_l - q\| \ge r_l$, and therefore the condition $\beta \ge 1 - \frac{\|c_l - q\|}{r_l}$ trivially holds if $\beta \ge 0$. Hence, $\zeta_1 = 0$ if and only if there exists $\beta \in \mathbb{R} \backslash \{1\}$ such that $\beta \ge 0$, $\beta \le 1 + \frac{\|c_l - q\|}{r_l}$, and $\beta(\|x_0 - q\| - \|c_l - q\|) \ge \|x_0 - q\|$. We distinguish two cases: (i) suppose that $\|x_0 - q\| - \|c_l - q\| \le 0$. Then, since $x_0 \ne q$, it follows that $\beta(\|x_0 - q\| - \|c_l - q\|) \ge \|x_0 - q\|$ can not

hold. Therefore, $\zeta_1 \ne 0$ and V_q and h_l are compatible in Γ; (ii) suppose instead that $\|x_0 - q\| - \|c_l - q\| > 0$. Then, $\zeta_1 = 0$ if and only if $\frac{\|x_0 - q\|}{\|x_0 - q\| - \|c_l - q\|} \le 1 + \frac{\|c_l - q\|}{r_l}$. Consequently, if $\frac{\|x_0 - q\|}{\|x_0 - q\| - \|c_l - q\|} > 1 + \frac{\|c_l - q\|}{r_l}$, then V_q and h_l are compatible in Γ. Consider then the case when $\frac{\|x_0 - q\|}{\|x_0 - q\| - \|c_l - q\|} \le 1 + \frac{\|c_l - q\|}{r_l}$ so that $\zeta_1 = 0$. Then, (7) reads

$$\zeta_2 := \min_{\beta \in \mathbb{R} \backslash \{1\}} \frac{1}{(\beta - 1)^2} \hat{\Phi}(\beta) \tag{14a}$$

$$\text{s.t. } \frac{\|x_0 - q\|}{\|x_0 - q\| - \|c_l - q\|} \le \beta \le 1 + \frac{\|c_l - q\|}{r_l}, \tag{14b}$$

where $\hat{\Phi}(\beta) = \beta(\alpha_l \|q - c_l\|^2 - \alpha_l r_l^2(1 - \beta)^2 - \beta(q - c_l)^T Q(q - c_l))$. By computing the roots of $\hat{\Phi}(\beta) = 0$, it follows that if $\beta_+ \ge 1 + \frac{\|c_l - q\|}{r_l}$, then $\hat{\Phi}(\beta) \ge 0$ for all $\beta \in [0, \beta_+]$, which implies that $\hat{\Phi}(\beta) \ge 0$ for all $\beta \in [\frac{\|x_0 - q\|}{\|x_0 - q\| - \|c_l - q\|}, 1 + \frac{\|c_l - q\|}{r_l}]$, from which it follows that $\zeta_2 \ge 0$ and V_q and h_l are compatible in Γ. $\square$

Proposition IV.7 provides a test for compatibility over a Lyapunov level set that only requires checking a set of algebraic conditions. Therefore, checking the compatibility of $V_q = \|x - q\|^2$ and $h_l(x) = \|x - c_l\|^2 - r_l^2$ over a Lyapunov sublevel set for a single integrator system can be done very efficiently.

D. Compatibility Verification for Higher Relative Degree Systems

Here we extend the results of Section IV-A to a larger class of system dynamics and barrier functions, specifically High-Order Control Barrier Functions (HOCBFs) [39]. Let $h : \mathbb{R}^n \to \mathbb{R}$ be a continuously differentiable function defining a safe set of the form (3). Consider the situation where h has to be differentiated $m \in \mathbb{Z}_{>0}$ times along the dynamics (1) until the control u appears explicitly (this is referred to as m being the relative degree of h under system (1), cf. [40]).

This means that, in order to ensure that the value of h remains positive at all times (i.e., $\mathcal{C}$ is positively invariant), we need to reason with its higher-order derivatives. To do so, given differentiable extended class $\mathcal{K}_\infty$ functions $\alpha^{(1)}, \alpha^{(2)}, \ldots, \alpha^{(m-1)}$, define a series of functions $\phi_0, \ldots, \phi_{m-1} : \mathbb{R}^n \to \mathbb{R}$ as follows: $\phi_0 = h$ and

$$\phi_i(x) = L_f \phi_{i-1}(x) + \alpha^{(i)}(\phi_{i-1}(x)), \quad i \in \{1, \ldots, m-1\}.$$

We further define sets $\mathcal{C}_1, \ldots, \mathcal{C}_m$ as $\mathcal{C}_1 = \mathcal{C}$ and

$$\mathcal{C}_i = \{x \in \mathbb{R}^n : \phi_{i-1}(x) \ge 0\}, \quad i \in \{2, \ldots, m\}.$$

The function h is a high-order control barrier function (HOCBF) of $\mathcal{C}$ if one can find differentiable, extended class $\mathcal{K}_\infty$ functions $\alpha^{(1)}, \alpha^{(2)}, \ldots, \alpha^{(m)}$ such that, for all $x \in \mathcal{C} \cap \mathcal{C}_2 \cap \ldots \cap \mathcal{C}_m$, there exists $u \in \mathbb{R}^m$ satisfying

$$L_f \phi_{m-1}(x) + L_g \phi_{m-1}(x)u + \alpha^{(m)}(\phi_{m-1}(x)) \ge 0. \tag{15}$$

If $m = 1$, this definition corresponds to the notion of CBF. According to [39, Theorem 5], any locally Lipschitz controller that satisfies (15) at each $x \in \mathcal{C} \cap \mathcal{C}_2 \cap \ldots \cap \mathcal{C}_m$ renders the set $\mathcal{C} \cap \mathcal{C}_2 \cap \ldots \cap \mathcal{C}_m$ positively invariant for system (1).

We next give an analogue of Definition II.4 for HOCBFs.

Definition IV.8. *(Compatibility of CLF-HOCBF pair): Let $\mathcal{D} \subset \mathbb{R}^n$ be open, $\mathcal{C} \subset \mathcal{D}$ be closed, V a CLF on $\mathcal{D}$ and h a HOCBF of $\mathcal{C}$. Then, V and h are compatible at $x \in \mathcal{C} \cap \mathcal{C}_2 \cap \ldots \cap \mathcal{C}_m$ if there exists $u \in \mathbb{R}^m$ satisfying (2) and (15) simultaneously. We refer to both functions as compatible in a set $\tilde{\mathcal{D}}$ if they are compatible at every point in $\tilde{\mathcal{D}}$.*

The following result is an analogue of Proposition IV.1 for the case when h is a HOCBF. Its proof follows an analogous argument and we omit it for space reasons.

Proposition IV.9. *(Characterization of CLF-HOCBF Compatibility): Given $q \in \mathcal{F}$, let $V_q : \mathbb{R}^n \to \mathbb{R}$ be a CLF of (1) with respect to q. Let h be a HOCBF of $\mathcal{C}$ with relative degree $m \in \mathbb{Z}_{>0}$. Let $W_q : \mathbb{R}^n \to \mathbb{R}$ be a positive definite function with respect to q and $\alpha^{(1)}, \alpha^{(2)}, \ldots, \alpha^{(m)}$ be differentiable extended class $\mathcal{K}_\infty$ functions. For $\Gamma \subset \mathcal{R}$, let*

$$\zeta_1 = \min_{x \in \Gamma, \beta \in \mathbb{R}} \|\beta L_g \phi_{m-1}(x) - L_g V_q(x)\|^2, \tag{16a}$$

$$s.t. \quad \beta \geq 0, \ \phi_i(x) \geq 0, \ i \in [m-1]. \tag{16b}$$

If $\zeta_1 \neq 0$, then V_q and h are compatible in $\Gamma \cap \mathcal{C} \cap \mathcal{C}_2 \cap \ldots \mathcal{C}_m$. Otherwise, if $\zeta_1 = 0$, let

$$\zeta_2 = \min_{x \in \Gamma, \beta \in \mathbb{R}} \tilde{\Phi}(x, \beta) \tag{17a}$$

$$s.t. \quad \beta \geq 0, \ \phi_i(x) \geq 0, \ i \in [m-1], \tag{17b}$$

where $\tilde{\Phi}(x, \beta) = -W_q(x) - L_f V_q(x) + \beta(L_f \phi_{m-1}(x) + \alpha^{(m)}(\phi_{m-1}(x)))$. If $\zeta_2 \geq 0$, then V_q and h are compatible in $\Gamma \cap \mathcal{C} \cap \mathcal{C}_2 \cap \ldots \mathcal{C}_m$. Conversely, if V_q and h are compatible in $\Gamma \cap \mathcal{C} \cap \mathcal{C}_2 \cap \ldots \mathcal{C}_m$, then there exists a set of differentiable extended class $\mathcal{K}_\infty$ functions $\alpha^{(1)}, \alpha^{(2)}, \ldots, \alpha^{(m)}$ and a positive definite function W_q with respect to q such that either $\zeta_1 \neq 0$ or $\zeta_1 = 0$ and $\zeta_2 \geq 0$.

To conclude this section, we consider the case of double-integrator dynamcs and circular obstacles. The double-integrator dynamics are given by

$$\begin{pmatrix} \dot{x} \\ \dot{v} \end{pmatrix} = \begin{pmatrix} \mathbb{0}_k & \mathbb{I}_k \\ \mathbb{0}_k & \mathbb{0}_k \end{pmatrix} \begin{pmatrix} x \\ v \end{pmatrix} + \begin{pmatrix} \mathbb{0}_k \\ \mathbb{I}_k \end{pmatrix} u, \tag{18}$$

with $k \in \mathbb{Z}_{>0}$ such that $n = 2k$, states $x \in \mathbb{R}^k$ and $v \in \mathbb{R}^k$, and input $u \in \mathbb{R}^k$. As pointed out in [41], only states of the form $(x_f, \mathbf{0}_k) \in \mathbb{R}^n$ are stabilizable for (18), and for any $x_f \in \mathbb{R}^k$, if we let $q = (x_f, \mathbf{0}_n)$, then $V_q : \mathbb{R}^n \to \mathbb{R}$ defined as $V_q(x, v) = \|x - x_f\|^2 + \|v\|^2 + (x - x_f)^T v$ is a CLF with respect to q. Next, consider $h : \mathbb{R}^n \to \mathbb{R}$ given by $h(x, v) = \|x - x_c\|^2 - r^2$, for some $x_c \in \mathbb{R}^k$ and $r > 0$. The following result shows that for this choice of V and h, (16) and (17) take a tractable form.

Proposition IV.10. *(CLF-HOCBF compatibility for circular obstacles and double integrator): Consider the double integrator dynamics (18). Let $q = (x_f, \mathbf{0}_k) \in \mathbb{R}^n$, and let $V_q(x, v) = \|x - x_f\|^2 + \|v\|^2 + (x - x_f)^T v$ be a CLF with respect to q, $W_q : \mathbb{R}^n \to \mathbb{R}$ a positive definite function with respect to q, and $h(x, v) = \|x - x_c\|^2 - r^2$ for some $x_c \in \mathbb{R}^k$, $r > 0$ a HOCBF. Let $\alpha_1 > 0$, $\alpha_2 > 0$, and $\phi_0 : \mathbb{R}^n \to \mathbb{R}$, $\phi_1 : \mathbb{R}^n \to \mathbb{R}$ defined as:*

$$\phi_0(x, v) = h(x),$$

$$\phi_1(x, v) = 2(x - x_c)^T v + \alpha_1(\|x - x_c\|^2 - r^2),$$

and $\mathcal{C}_1 = \{(x, v) \in \mathbb{R}^{2n} : \phi_1(x, v) \geq 0\}$. For $\Gamma \subset \mathcal{R}$, let

$$\hat{\zeta}_1 = \min_{x \in \Gamma, \beta \in \mathbb{R}, \tilde{x} \in \mathbb{R}^k} \|2\tilde{x} - 2v - (x - x_f)\|^2, \tag{19a}$$

$$s.t. \quad \beta \geq 0, \ \phi_i(x) \geq 0, \ i \in \{0, 1\}, \tag{19b}$$

$$\beta(x - x_c) - \tilde{x} \leq 0, \ \tilde{x} - \beta(x - x_c) \leq 0. \tag{19c}$$

If $\hat{\zeta}_1 \neq 0$, then V_q and h are compatible in $\Gamma \cap \mathcal{C} \cap \mathcal{C}_1$. Otherwise, if $\hat{\zeta}_1 = 0$, let

$$\hat{\zeta}_2 = \min_{\substack{(x,v) \in \Gamma, \beta \in \mathbb{R}, \\ \tilde{x} \in \mathbb{R}^k, \tilde{v} \in \mathbb{R}^k}} \hat{\Phi}(x, v, \tilde{x}, \tilde{v}) \tag{20a}$$

$$s.t. \quad \beta \geq 0, \ \phi_i(x) \geq 0, \ i \in \{0, 1\}, \tag{20b}$$

$$2\tilde{x} - 2v + x - x_f \leq 0, \tag{20c}$$

$$-2\tilde{x} + 2v - (x - x_f) \leq 0, \tag{20d}$$

$$\beta(x - x_c) - \tilde{x} \leq 0, \ \tilde{x} - \beta(x - x_c) \leq 0, \tag{20e}$$

$$\beta v - \tilde{v} \leq 0, \ -\beta v + \tilde{v} \leq 0, \tag{20f}$$

where $\hat{\Phi}(x, v, \tilde{x}, \tilde{v}) = 2\tilde{v}^T v + \alpha_1 \tilde{x}^T v + 2\alpha_2 \tilde{x}^T v + \alpha_2 \alpha_1 \tilde{x}^T (x - x_c) - \alpha_1 \alpha_2 r^2 \beta - 2(x - x_f)^T v - \|v\|^2 - W_q(x, v)$. If $\hat{\zeta}_2 \geq 0$, then V_q and h are compatible in $\Gamma \cap \mathcal{C} \cap \mathcal{C}_1$.

Proof. The result follows from Proposition IV.9 and by introducing the new variables $\tilde{x} = \beta(x - x_c)$, $\tilde{v} = \beta v$. $\square$

Note that (19) is a QCQP, and if W_q is quadratic, (20) is also a QCQP and can therefore be solved efficiently [38].

V. C-CLF-CBF-RRT

In this section, we introduce a novel motion planning algorithm, termed Compatible-CLF-CBF-RRT (C-CLF-CBF-RRT), that leverages the compatibility results from Section IV to generate collision-free paths that can be tracked using CLF-CBF based controllers.

A. CLF-CBF Compatible Paths

We start by defining formally the type of paths that we seek to find using our motion planning algorithm. Intuitively, a path is *CLF-CBF compatible* if the CLF-CBF controller (5) successfully connects pairs of consecutive waypoints in the path.

Definition V.1. *(CLF-CBF Compatible Path): Let $\mathcal{A} = \{x_i\}_{i=1}^{N_a} \subset \mathcal{F}$ be a sequence of points, with $N_a \in \mathbb{Z}_{>0}$, $x_1 = x_{init}$ and $x_{N_a} \in \mathcal{X}_{goal} := \mathcal{B}(x_{goal}, \delta_{goal})$, where $x_{goal} \in \mathbb{R}^n$ and $\delta_{goal} > 0$. $\mathcal{A}$ is a CLF-CBF compatible path if for each $i \in [N_a - 1]$,*

(i) *there exists a CLF $V_i : \mathbb{R}^n \to \mathbb{R}_{\geq 0}$ with respect to x_{i+1} in an open set containing $\Gamma_i := \{x \in \mathbb{R}^n : V_i(x) \leq V_i(x_i)\}$ for system (1);*

(ii) *there exist extended class $\mathcal{K}_\infty$ functions $\{\alpha_{i,l} : \mathbb{R} \to \mathbb{R}\}_{l \in [M]}$ and positive definite functions $W_i : \mathbb{R}^n \to \mathbb{R}_{\geq 0}$ with respect to x_{i+1} such that the optimization problem*

$$\min_{u \in \mathbb{R}^m} \frac{1}{2} \|u\|^2 \tag{21}$$

$$s.t. \ L_f h_{j,l}(x) + L_g h_{j,l}(x) u \geq -\alpha_{i,l}(h_{j,l}(x)),$$

$$\forall j \in \mathcal{I}_l(x), l \in [M],$$
$$L_f V_i(x) + L_g V_i(x) u + W_i(x) \le 0.$$

is feasible for all $x \in \Gamma_i \cap \mathcal{F}$.

For each $i \in [N_a - 1]$, let $u_i^* : \Gamma_i \cap \mathcal{F} \to \mathbb{R}^m$ be a function mapping each $x \in \Gamma_i \cap \mathcal{F}$ to the solution of (21). Under the assumption that u_i^* is locally Lipschitz, cf. Remark IV.5, the feasibility of (21) ensures that the solution of the closed-loop system $\dot{x} = f(x) + g(x) u_i^*(x)$ with initial condition at x_i is collision-free and asymptotically converges to x_{i+1}. Therefore, CLF-CBF compatible paths guarantee that the controller obtained by solving (21) for each waypoint steers an agent obeying the dynamics (1) towards the next waypoint while remaining collision-free. Even though the convergence to the waypoint x_{i+1} is only achieved in infinite time, one can execute the controller u_i^* until the agent is sufficiently close to x_{i+1} and then switch to the next controller u_{i+1}^*. We elaborate more on this point in Section VI, where we identify conditions on the CLF-CBF compatible path under which the controllers $\{u_i^*\}_{i=1}^{N_a - 1}$ can steer the agent from a neighborhood of each waypoint to a neighborhood of the next one.

Remark V.2. *(Controllability Requirements for CLF-CBF Compatible Paths):* Definition V.1 requires each of the points in the path $\mathcal{A}$ to be asymptotically stabilizable. This condition imposes some structural properties on the class of systems that admit such paths, which we examine next:

Fully actuated systems: In the case when $m = n$ and $g(x)$ is invertible for all $x \in \mathbb{R}^n$, CLF-CBF compatible paths exist because any point $q \in \mathbb{R}^n$ is asymptotically stabilizable. Indeed, in this setting the function $V_q : \mathbb{R}^n \to \mathbb{R}$ defined by $V_q(x) = \frac{1}{2} \|x - q\|^2$ is a CLF with respect to q;

Underactuated systems: In the case when $m < n$, the set of stabilizable points is limited. For instance, for linear systems with $f(x) = Ax$ and $g(x) = B$, with $A \in \mathbb{R}^{n \times n}$ and $B \in \mathbb{R}^{n \times m}$, only the points $q \in \mathbb{R}^n$ such that $Aq \in \text{Im}(B)$ are stabilizable. This is not a major restriction in a lot of cases of interest. For example, for a double-integrator system, where $m = k$ and $n = 2k$, with $k \in \mathbb{Z}_{>0}$, and

$$A = \begin{pmatrix} \mathbb{0}_k & \mathbb{I}_k \\ \mathbb{0}_k & \mathbb{0}_k \end{pmatrix}, \quad B = \begin{pmatrix} \mathbb{0}_k \\ \mathbb{I}_k \end{pmatrix},$$

this condition restricts the set of stabilizable points to those that have a zero velocity, but arbitrary position, as pointed out in Section IV-D. In general, if $m < n$, there often exists a smooth change of coordinates $\psi : \mathbb{R}^n \to \mathbb{R}^m$ that transforms the dynamics into a single integrator in $\mathbb{R}^m$. In [42, Section IV.A] and [43], for instance, this is achieved for unicycle dynamics, by taking the transformation $\psi(x_1, x_2, \theta) = [x_1 + l\cos(\theta), x_2 + l\sin(\theta)]$ (where $l > 0$ is a positive design parameter). Then, for any $q \in \text{Im}(\psi)$, the set $M_q = \{x \in \mathbb{R}^n : \psi(x) = q\}$ can be asymptotically stabilized. Therefore, if $m < n$ but such a transformation ψ exists, Definition V.1 can be adapted so that the points in $\mathcal{A}$ are in sets of the form M_q. ●

B. Algorithm Description

In this section we introduce the `C-CLF-CBF-RRT` algorithm, which builds upon RRT, cf. Section II-C, and generates CLF-CBF compatible paths. Algorithm 2 presents the pseudocode description.

Algorithm 2 `C-CLF-CBF-RRT`

1: **Parameters**: $\mathcal{R}, x_{\text{init}}, \mathcal{X}_{\text{goal}}, k, \tau, \eta, \{h_l, \alpha_l\}_{l=1}^M$
2: $\mathcal{T}.\text{init}(x_{\text{init}})$
3: **for** $i \in [1, \ldots, k]$ **do**
4:     $x_{\text{rand}} \leftarrow$ RANDOM_STATE()
5:     $x_{\text{near}} \leftarrow$ NEAREST_NEIGHBOR$(x_{\text{rand}}, \mathcal{T})$
6:     $x_{\text{new}} \leftarrow$ NEW_STATE$(x_{\text{rand}}, x_{\text{near}}, \eta)$
7:     **if** not FREE_SPACE(x_{new}) **then**
8:       **skip to next iteration**
9:     **end if**
10:     $V, W \leftarrow$ FIND_CLF(x_{new})
11:     **if** COMPATIBILITY$(x_{\text{near}}, x_{\text{new}}, \tau, \{h_l, \alpha_l\}_{l=1}^M, V, W)$ **then**
12:         $\mathcal{T}.\text{add\_vertex}(x_{\text{new}})$
13:         $\mathcal{T}.\text{add\_edge}(x_{\text{near}}, x_{\text{new}})$
14:         **if** $x_{\text{new}} \in \mathcal{X}_{\text{goal}}$ **then**
15:             **return** $\mathcal{T}$
16:         **end if**
17:     **end if**
18: **end for**
19: **return** $\mathcal{T}$

The input for `C-CLF-CBF-RRT` consists of a compact, convex set $\mathcal{R} \subset \mathbb{R}^n$, an initial configuration $x_{\text{init}} \in \mathbb{R}^n$, a goal region $\mathcal{X}_{\text{goal}} \subset \mathbb{R}^n$, the number of iterations $k \in \mathbb{Z}_{>0}$ of the algorithm, the number of iterations $\tau \in \mathbb{Z}_{>0}$ for the compatibility check, a set of extended class $\mathcal{K}_\infty$ functions $\{\alpha_l\}_{l=1}^M$, the steering parameter $\eta > 0$, and a set of obstacles $\{\mathcal{O}_l\}_{l=1}^M$ defined by functions $h_l : \mathbb{R}^n \to \mathbb{R}$ for $l \in [M]$. At the beginning, a tree $\mathcal{T}$ is initialized with a single node at x_{init} and no edges.

The `C-CLF-CBF-RRT` algorithm operates similarly to the `GEOM-RRT` algorithm described in Section II-C.

At each iteration, steps 4:-6: are the same as in Algorithm 1. In general, RANDOM_STATE samples $\mathcal{R}$ uniformly, but if we know that only a subset of the points in $\mathcal{R}$ is stabilizable, one can choose to sample uniformly only over such points. The functions NEAREST_NEIGHBOR and NEW_STATE operate identically to how they do in `GEOM-RRT`. We note that, since $\mathcal{R}$ is convex, x_{new} is guaranteed to belong to it. Next, the function FREE_SPACE checks whether $x_{\text{new}} \in \mathcal{F}$. If $x_{\text{new}} \notin \mathcal{F}$, it skips to the next iteration. Otherwise, FIND_CLF finds a CLF V and associated positive definite function W with respect to x_{new}. Then, the COMPATIBILITY function checks whether there exists a CLF-CBF based controller that steers the system from x_{near} to x_{new}. If the COMPATIBILITY function returns a value of True, then x_{new} is added as a vertex to $\mathcal{T}$ and is connected by an edge from x_{near}. If $x_{\text{new}} \in \mathcal{X}_{\text{goal}}$, there exists a single path in $\mathcal{T}$ from x_{init} to x_{new}.

Regarding the search for a control Lyapunov function with `FIND_CLF`, beyond what we noted in Remark V.2, one can also use a variety of tools from the literature, such as sum-of-squares techniques [44] or neural networks [45]. In Section V-C, we discuss in detail the definition of `COMPATIBILITY` function.

Remark V.3. *(Sampling in Underactuated Systems):* A requirement for step 7: of Algorithm 2 to return a value of `True` is that x_{new} is stabilizable. Since this point is obtained through random sampling, in general this might not be the case. However, if we know the set of points that are stabilizable (for instance, an m-dimensional manifold $\mathcal{M}$ in the case of underactuated systems with m controls, cf. Remark V.2), then we can project x_{new} onto such set. •

C. The COMPATIBILITY function

Here we define the operation of the `COMPATIBILITY` function. Given the CLF V and the positive definite function W with respect to x_{new} found by `FIND_CLF`, it checks whether the optimization problem

$$\min_{u \in \mathbb{R}^m} \frac{1}{2} \|u\|^2, \tag{22}$$
$$\text{s.t. } L_f h_{j,l}(x) + L_g h_{j,l}(x)u \geq -\alpha_l(h_{j,l}(x)),$$
$$\forall j \in \mathcal{I}_l(x), l \in [M],$$
$$L_f V(x) + L_g V(x)u + W(x) \leq 0.$$

is feasible for all $x \in \Theta \cap \mathcal{F}$, where $\Theta = \{x \in \mathbb{R}^n : V(x) \leq V(x_{\text{near}})\}$ and α_l is the class $\mathcal{K}_\infty$ function associated with h_l.

1. Find obstacles that intersect domain of interest: To check whether (22) is feasible, we first find the obstacles that intersect Θ, i.e., we find $l \in [M]$ such that $\text{Cl}(\mathcal{O}_l) \cap \Theta \neq \emptyset$. This can be done by solving the following optimization problem for every $l \in [M]$:

$$\min_{x \in \mathbb{R}^n} V(x) \tag{23}$$
$$\text{s.t. } h_{i,l}(x) \leq 0, \quad \forall i \in [N_l].$$

Then, $\text{Cl}(\mathcal{O}_l) \cap \Theta \neq \emptyset$ if and only if the optimal value of (23) is smaller than or equal to $V(x_{\text{near}})$. Problem (23) is tractable, for instance, under the settings considered in Section IV, where V is quadratic and the constraints are affine (in which case (23) is a quadratic program) or ellipsoidal (in which case (23) is a QCQP).

2. Reduce number of constraints and check for compatibility: Next, we reduce the number of constraints in (22) to $\mathcal{L} := \{l \in [M] : \Theta \cap \text{Cl}(\mathcal{O}_l)\}$ (Lemma A.1 ensures this step retains consistency). Then, `COMPATIBILITY` uses Proposition IV.1 for each $l \in \mathcal{L}$. First, for each $l \in \mathcal{L}$, it solves the optimization problem (6) with $\Gamma = \Theta$ and obtains the value $\zeta_{1,l}$. If $\zeta_{1,l} = 0$, it solves (7) with $\Gamma = \Theta$ and obtains the value $\zeta_{2,l}$. If for all $l \in \mathcal{L}$, the obtained values of $\zeta_{1,l}$ and $\zeta_{2,l}$ are such that $\zeta_{1,l} \neq 0$ or $\zeta_{1,l} = 0$ and $\zeta_{2,l} \geq 0$, then V and h_l are compatible in $\Theta \cap \mathcal{F}$ for all $l \in \mathcal{L}$ and `COMPATIBILITY` returns `True`.

3. If unsuccessful, increase feasibility set and recheck: Otherwise, it updates the set of extended class $\mathcal{K}_\infty$ functions and the function W in a way that increases the feasible set of (22), and performs again the same check about its

feasibility. In every subsequent iteration, we use a new W obtained by multiplying the previous one by a constant factor $\sigma \in (0,1)$, and use linear extended class $\mathcal{K}_\infty$ functions $\alpha_l(s) = \alpha_{0,l}s$ with the parameter $\alpha_{0,l}$ being multiplied by a constant factor greater than 1 at every iteration. With this choice, the objective function Φ of (7) does not decrease at any point, which means that the value of ζ_1 remains the same but the condition $\zeta_2 \geq 0$ becomes easier to satisfy, which makes it easier for `COMPATIBILITY` to return a value of `True`. If after τ of those updates the function still has not returned a value of `True`, it returns a value of `False`.

VI. ANALYSIS OF C-CLF-CBF-RRT

In this section we establish the probabilistic completeness of `C-CLF-CBF-RRT`. We do this by first showing that if `C-CLF-CBF-RRT` returns a tree with a vertex in $\mathcal{X}_{\text{goal}}$, then this tree contains a CLF-CBF compatible path; and then showing that, under suitable conditions, `C-CLF-CBF-RRT` in fact returns a tree with a vertex in $\mathcal{X}_{\text{goal}}$ with high probability.

Proposition VI.1. *(C-CLF-CBF-RRT and CLF-CBF Compatible Path): Suppose that `C-CLF-CBF-RRT` returns a tree $\mathcal{T}$ that contains a vertex $q_{\text{goal}} \in \mathcal{X}_{\text{goal}}$. Then, the single path in $\mathcal{T}$ from x_{init} to q_{goal} is CLF-CBF compatible.*

Proof. Let $N_a \in \mathbb{Z}_{>0}$ and $\mathcal{A} = \{x_i\}_{i=1}^{N_a}$ be the path obtained from `C-CLF-CBF-RRT`, with $x_1 = x_{\text{init}}$ and $x_{N_a} \in \mathcal{X}_{\text{goal}}$. First, `FREE_SPACE` ensures that $x_i \in \mathcal{F}$ for all $i \in [N_a]$. Moreover, `FIND_CLF` ensures that, for all $i \in [N_a - 1]$, there exists a CLF V_i with respect to x_{i+1}, and `COMPATIBILITY` ensures that there exists a set of class $\mathcal{K}_\infty$ functions $\{\alpha_{i,l}\}_{l=1}^M$ and a positive definite function W_i with respect to x_{i+1} such that the optimization problem (21) is feasible for all points in the set $\{x \in \mathbb{R}^n : V_i(x) \leq V_i(x_i)\} \cap \mathcal{F}$. This ensures that $\mathcal{A}$ is CLF-CBF compatible. $\square$

We next show that, under some extra assumptions, `C-CLF-CBF-RRT` returns a tree with a vertex in $\mathcal{X}_{\text{goal}}$ with probability one as the number of iterations k goes to infinity. In doing so, our next result is critical as it provides conditions under which there exist neighborhoods around a CLF-CBF compatible path for which points of two consecutive neighborhoods can be connected with a CLF-CBF-based controller.

Lemma VI.2. *(Compatibility in Neighboring Vertices): Let $\mathcal{A} = \{x_i\}_{i=1}^{N_a}$, $N_a \in \mathbb{Z}_{>0}$, be a CLF-CBF compatible path such that there exists $\delta_{\text{clear}} > 0$ with $\mathcal{B}(x_i, \delta_{\text{clear}}) \subset \mathcal{F}$ for all $i \in \{2, \ldots, N_a\}$. Let $\mathcal{N}_1 = \{x_{\text{init}}\}$. For each $i \in \{2, \ldots, N_a\}$, assume that there exist sets $\mathcal{N}_i$, with $x_i \in \mathcal{N}_i$, and $\hat{\Gamma}_i$, with $\Gamma_i \subset \hat{\Gamma}_i$ (and Γ_i defined as in Definition V.1), satisfying the following properties:*

(i) *for each $y \in \mathcal{N}_i$, there exists a CLF $V_y : \hat{\Gamma}_i \to \mathbb{R}$ with respect to y in $\hat{\Gamma}_i$ (with associated positive definite function W_y) and a bounded controller $\hat{u}_y : \hat{\Gamma}_i \to \mathbb{R}^m$ satisfying the corresponding CLF condition in $\hat{\Gamma}_i$;*

(ii) *there exists a bounded controller $u_i^* : \hat{\Gamma}_i \cap \mathcal{F} \to \mathbb{R}^m$ that satisfies the constraints in (21) for all points in $\hat{\Gamma}_i$ and, for each $y \in \mathcal{N}_i$,*

$$|(\nabla V_y(x) - \nabla V_i(x))^T (f(x) + g(x)u_i^*(x))|$$

$$< W_i(x), \quad (24)$$

for all $x \in \mathcal{Z} = \{z \in \mathcal{F} \ : \ \exists l \in [M] \text{ s.t. } d(z, \mathcal{O}_l) \leq \frac{\delta_{clear}}{2}\}$;

(iii) *for each* $y_2 \in \mathcal{N}_i$ *and* $y_1 \in \mathcal{N}_{i-1}$, $\Gamma_{y_1, y_2} := \{x \in \mathbb{R}^n : V_{y_2}(x) \leq V_{y_2}(y_1)\} \subset \hat{\Gamma}_i$;

(iv) *whenever* $x_{new} \in \mathcal{N}_i$, *global solutions to the optimization problems* (6) *and* (7) *in* COMPATIBILITY *are found.*

Then, for each $i \in \{2, \ldots, N_a\}$, $y_2 \in \mathcal{N}_i$, *and* $y_1 \in \mathcal{N}_{i-1}$, *there exists a set of extended class* $\mathcal{K}_\infty$ *functions* $\{\bar{\alpha}_{i,l}\}_{l=1}^M$ *and* $\bar{\sigma} > 0$ *(both dependent on* y_1, y_2*) such that, by taking* $W_{y_2}^{\bar{\sigma}}(x) = \bar{\sigma} W_{y_2}(x)$, *it holds that* COMPATIBILITY$(y_1, y_2, 1, \{h_l, \bar{\alpha}_{i,l}\}_{l=1}^M, V_{y_2}, W_{y_2}^{\bar{\sigma}})$ = True.

Proof. Given $i \in \{2, \ldots, N_a\}$, $y_2 \in \mathcal{N}_i$, and $y_1 \in \mathcal{N}_{i-1}$, our goal is to show that there exists a set of extended class $\mathcal{K}_\infty$ functions $\{\bar{\alpha}_{i,l}\}_{l=1}^M$ and a sufficiently small $\bar{\sigma} > 0$ such that

$$\min_{u \in \mathbb{R}^m} \frac{1}{2} \|u\|^2, \quad (25)$$
$$\text{s.t. } L_f h_{j,l}(x) + L_g h_{j,l}(x)u \geq -\bar{\alpha}_{i,l}(h_{j,l}(x)),$$
$$\forall j \in \mathcal{I}_l(x), l \in [M],$$
$$\nabla V_{y_2}(x)^T(f(x) + g(x)u) + \bar{\sigma} W_{y_2}(x) \leq 0,$$

is feasible for all $x \in \Gamma_{y_1, y_2} \cap \mathcal{F}$. Figure 1 provides a visual aid for the argument that follows. The set Γ_{y_1, y_2} is depicted in red, the sets $\mathcal{N}_i$ in blue, $\mathcal{Z}$ in light purple, and the obstacles $\{\mathcal{O}_l\}_{l=1}^M$ in green. For convenience, we let $T_{y_1, y_2} = \Gamma_{y_1, y_2} \cap \mathcal{Z}$ (depicted in dark purple).

Feasibility on $(\Gamma_{y_1, y_2} \backslash T_{y_1, y_2}) \cap \mathcal{F}$: Since T_{y_1, y_2} contains all points that are closer than $\frac{\delta_{clear}}{2}$ from the boundary, there exists $h_0 > 0$ such that $h_{j,l}(x) > h_0$ for all $x \in (\Gamma_{y_1, y_2} \backslash T_{y_1, y_2}) \cap \mathcal{F}$, $l \in [M]$ and $j \in \mathcal{I}_l(x)$. Therefore, by taking $\alpha_{i,l}^* > 0$, with

$$\alpha_{i,l}^* > \frac{\displaystyle\sup_{\substack{x \in (\Gamma_{y_1,y_2} \backslash T_{y_1,y_2}) \cap \mathcal{F}, \\ j \in \mathcal{I}_l(x)}} |L_f h_{j,l}(x) + L_g h_{j,l}(x)\hat{u}_{y_2}(x)|}{h_0},$$

for each $l \in [M]$ (which exists because $\hat{u}_{y_2}$ is bounded on $\hat{\Gamma}_i$ by (i)), it holds that

$$L_f h_{j,l}(x) + L_g h_{j,l}(x)\hat{u}_{y_2}(x) + \alpha_{i,l}^* h_{j,l}(x) \geq 0,$$
$$\forall j \in \mathcal{I}_l(x), l \in [M],$$
$$\nabla V_{y_2}(x)^T(f(x) + g(x)\hat{u}_{y_2}(x)) + \sigma W_{y_2}(x) \leq 0,$$

for all $x \in (\Gamma_{y_1, y_2} \backslash T_{y_1, y_2}) \cap \mathcal{F}$ and $\sigma \in (0, 1)$, where we have used that $\hat{u}_{y_2}$ satisfies the CLF condition for V_{y_2} by (i).

Feasibility on T_{y_1, y_2}: From (ii), there exists a bounded controller u_i^* satisfying the constraints in (21) for all $x \in \hat{\Gamma}_i$. Since $\Gamma_{y_1, y_2} \subset \hat{\Gamma}_i$, cf. (iii), u_i^* satisfies the constraints in (21) for all $x \in \Gamma_{y_1, y_2}$. Moreover, since (24) holds for all $x \in \mathcal{Z}$ (note that this is only possible because $\mathcal{B}(x_i, \delta_{clear}) \subset \mathcal{F}$ and therefore $x_i \notin \mathcal{Z}$, which means that the right-hand side of (24) is strictly positive), by (ii) it follows that

$$\nabla V_{y_2}(x)^T(f(x) + g(x)u_i^*(x)) < 0,$$

for all $x \in T_{y_1, y_2}$. Since $\mathcal{Z}$ is compact, this implies that there exists $\bar{\sigma} \in (0, 1)$ sufficiently small such that

$$L_f h_{j,l}(x) + L_g h_{j,l}(x)u_i^*(x) + \alpha_{i,l}(h_{j,l}(x)) \geq 0,$$

$$\forall j \in \mathcal{I}_l(x), l \in [M],$$
$$\nabla V_{y_2}(x)^T(f(x) + g(x)u_i^*(x)) + \bar{\sigma} W_{y_2}(x) \leq 0.$$

for all $x \in T_{y_1, y_2}$.

Hence, by taking $\bar{\alpha}_{i,l}$ as an extended class $\mathcal{K}_\infty$ function such that $\bar{\alpha}_{i,l}(s) > \max\{\alpha_{i,l}(s), \alpha_{i,l}^* s\}$ for all $s \geq 0$, and $\bar{\sigma} \in (0, 1)$ sufficiently small as described above, (25) is feasible for all $x \in \Gamma_{y_1, y_2} \cap \mathcal{F}$. Since COMPATIBILITY finds the global solutions of the optimization problems (6) and (7), cf. (iv), it follows that COMPATIBILITY$(y_1, y_2, 1, \{h_l, \bar{\alpha}_{i,l}\}_{l=1}^M, V_{y_2}, W_{y_2}^{\bar{\sigma}})$ = True (note that since (25) includes CBF constraints for $l \in [M]$, this argument is valid independently of the set $\mathcal{L}$ found by solving (23)). $\qquad \square$
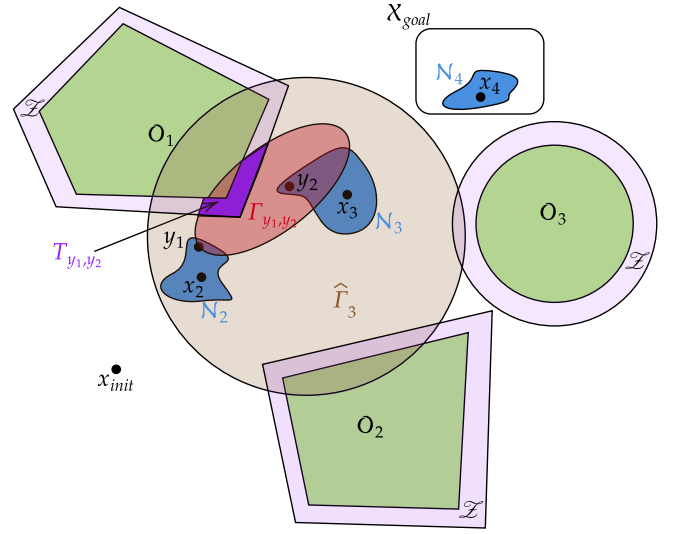

Fig. 1: Visual aid for the arguments described in the proof of Lemma VI.2.

Remark VI.3. (*Verification of Assumptions of Lemma VI.2 for Specific Classes of Systems*): For *fully actuated systems*, the set $\mathcal{N}_i$ in Lemma VI.2 can be taken as a ball centered at the waypoint x_i. As mentioned in Remark V.2, for such systems, $V_y(x) = \frac{1}{2}\|x - y\|^2$ is a CLF for any $y \in \mathbb{R}^n$. Moreover, we can take $W_y(x) = \|x - y\|^2$ and the controller $\hat{u} : \mathbb{R}^n \to \mathbb{R}^n$ defined as $\hat{u}(x) = -\frac{(x-y_2)^T f(x) + \|x - y_2\|^2}{\|g(x)^T(x-y_2)\|^2} g(x)^T(x - y_2)$ is such that $(x - y_2)^T(f(x) + g(x)\hat{u}(x)) + \|x - y_2\|^2 \leq 0$ for all $x \in \Gamma_{y_1, y_2}$ and is bounded, since

$$\|\hat{u}(x)\| \leq \frac{\|x - y_2\| \, (\|f(x)\| + \|x - y_2\|)}{\|g(x)^T(x - y_2)\|}$$
$$\frac{\|g(x)^{-1}g(x)(x - y_2)\| \, (\|f(x)\| + \|x - y_2\|)}{\|g(x)^T(x - y_2)\|}$$
$$\leq \|g(x)^{-1}\| \, \|x - y_2\|.$$

Given that an explicit expression for the CLF is available, the conditions (ii), (iii) in Lemma VI.2 can be verified directly and one can choose the radius of the balls defining $\mathcal{N}_i$ to satisfy them. Furthermore, Propositions IV.6 and IV.7 provide two settings where condition (iv) holds.

A similar argument can be made for the *double integrator* in dimension $2k \in \mathbb{Z}_{>0}$. As mentioned in Remark V.2, in

that case only the points of the form $(x_f, \mathbf{0}_k) \in \mathbb{R}^{2k}$ are stabilizable. Hence, the sets $\mathcal{N}_i$ in Lemma VI.2 can be taken in the form $\mathcal{N}_i := \{(x, \mathbf{0}_k) \in \mathbb{R}^{2k} : \|x - x_f\| < \nu_i\}$ for some $\nu_i > 0$. Furthermore, one can use the explicit expression of the CLF provided in Section IV-D and choose the parameters ν_i in order to verify the rest of the assumptions in Lemma VI.2. ●

In general, if the neighborhood $\mathcal{N}_i$ around x_i in Lemma VI.2 is sufficiently small and ∇V_y is continuous in y (with the assumption that $V_{x_i} = V_i$), the left-hand side of (24) can be made sufficiently small so that the inequality holds. Note that Assumptions (i), (iii), and (iv) are not restrictive and hold in several cases of interest, as outlined in Remark VI.3. Overall, the assumptions in Lemma VI.2 ensure that there exist neighborhoods around every waypoint of a CLF-CBF compatible path such that the controller obtained as the solution of (21) can connect a point from each neighborhood to any point in the neighborhood of the next waypoint. We next leverage this property to show the probabilistic completeness of C-CLF-CBF-RRT.

Proposition VI.4. *(Probabilistic Completeness of C-CLF-CBF-RRT): Suppose that there exists a CLF-CBF compatible path $\mathcal{A} = \{x_i\}_{i=1}^{N_a}$, $N_a \in \mathbb{Z}_{>0}$, and suppose that all the assumptions in Lemma VI.2 regarding $\mathcal{A}$ hold. Further suppose that*

(i) *there exists a positive probabiliy p_i that RANDOM_STATE returns a point from $\mathcal{N}_i$;*

(ii) *for each $y \in \mathcal{N}_i$, FIND_CLF returns V_y and W_y (as defined in item (i) of Lemma VI.2);*

(iii) *the extended class $\mathcal{K}_\infty$ functions $\{\alpha_{i,l}\}_{i\in[N_a], l\in[M]}$ in (21) are upper bounded by linear extended class $\mathcal{K}_\infty$ functions, i.e., there exist $\hat{\alpha}_{i,l} > 0$ for $i \in [N_a]$ and $l \in [M]$ such that $\alpha_{i,l}(s) \leq \hat{\alpha}_{i,l}s$ for all $s \geq 0$;*

(iv) *the steering parameter η in NEW_STATE is such that*
$$\eta > \max_{i \in [N_a - 1]} \max_{y_2 \in \mathcal{N}_{i+1}, y_1 \in \mathcal{N}_i} \|y_2 - y_1\|.$$

Then, there exists $\tau^* \in \mathbb{Z}_{>0}$ such that if $\tau > \tau^*$, the probability of C-CLF-CBF-RRT (executed with parameters τ, η, and any set of extended class $\mathcal{K}_\infty$ functions $\{\alpha_l\}_{l\in[M]}$) returning a tree without a vertex in $\mathcal{X}_{goal}$ tends to zero as the number of iterations k goes to infinity.

Proof. The proof follows a similar reasoning to [35, Theorem 1] that proves probabilistic completeness for GEOM-RRT. Let $i \in [N_a - 1]$. First, we show that if $\mathcal{N}_i$ contains a vertex x_{near} from the tree $\mathcal{T}$ in C-CLF-CBF-RRT, then with probability $p_i > 0$ in the next iteration a vertex will be added from $\mathcal{N}_{i+1}$. To see this, note that by assumption there exists a probability $p_i > 0$ that the function RANDOM_STATE returns a point x_{rand} from $\mathcal{N}_{i+1}$. Given (iv), the distance between $x_{\text{near}} \in \mathcal{N}_i$ and $x_{\text{rand}} \in \mathcal{N}_{i+1}$ is less than η, and therefore $x_{\text{new}} = x_{\text{rand}}$. Now, Lemma VI.2 ensures that there exists a set of extended class $\mathcal{K}_\infty$ functions $\{\bar{\alpha}_{i,l}\}_{l=1}^M$, a CLF $V_{x_{\text{rand}}}$ with respect to x_{rand} and a positive definite function $W_{x_{\text{rand}}}^{\bar{\sigma}}$ with respect to x_{rand} such that COMPATIBILITY$(x_{\text{near}}, x_{\text{rand}}, \tau, \{h_l, \bar{\alpha}_{i,l}\}_{l=1}^M, V_{x_{\text{rand}}}, W_{x_{\text{rand}}}^{\bar{\sigma}})$ returns True. Moreover, since the functions $\{\alpha_{i,l}\}_{l=1}^M$ are upper bounded by linear extended class $\mathcal{K}_\infty$ functions with slopes $\{\hat{\alpha}_{i,l}\}_{l=1}^M$, by performing the updates in the extended class $\mathcal{K}_\infty$ functions described in Section V-C.3,

it follows that there exists τ^* sufficiently large such that if $\tau > \tau^*$, the updated linear extended class $\mathcal{K}_\infty$ functions used in COMPATIBILITY have slopes larger than $\{\hat{\alpha}_{i,l}\}_{l=1}^M$ respectively and the coefficient multiplying $W_{x_{\text{rand}}}$ is smaller than $\bar{\sigma}$, which makes the COMPATIBILITY function return True. This means that x_{rand} is added to $\mathcal{T}$ with the corresponding edge from x_{near} to x_{rand}, as stated.

Next, in order for C-CLF-CBF-RRT to reach $\mathcal{X}_{\text{goal}}$ from x_{init}, the algorithm needs to successively select points from $\mathcal{N}_{i+1}$ as described previously for $i \in [N_a - 1]$. For k iterations of C-CLF-CBF-RRT, this stochastic process can be described as k Bernouilli trials [46, Definition 2.5] with success probabilities $\{p_i\}_{i=1}^{N_a - 1}$. The algorithm reaches $\mathcal{X}_{\text{goal}}$ from x_{init} after $N_a - 1$ successful outcomes. Let $p := \min_{i \in [N_a - 1]} p_i$. Using the same argument as in [35, Theorem 1], the probability that this stochastic process does not have $N_a - 1$ successful outcomes after k iterations is smaller than $\frac{(N_a-1)!}{(N_a-2)!}k^{N_a-1}e^{-pk}$. This means that the probability of C-CLF-CBF-RRT returning a tree without a vertex in $\mathcal{X}_{\text{goal}}$ tends to zero as the number of iterations k goes to infinity. □

Remark VI.5. *(Verification of Assumptions of Proposition VI.4):* As mentioned in Remark VI.3, for *fully actuated systems* the set $\mathcal{N}_i$ in Lemma VI.2 can be taken as a ball centered at the waypoint x_i. If RANDOM_STATE samples $\mathcal{R}$ uniformly, it returns a point in such ball with probability equal to its relative volume in $\mathcal{R}$. Furthermore, in this case FIND_CLF can simply return $V_y(x) = \frac{1}{2}\|x - y\|^2$ and $W_y(x) = \|x - y\|^2$ for any $y \in \mathcal{N}_i$. For the *double integrator* in dimension $2k \in \mathbb{Z}_{>0}$, as mentioned in Remark VI.3, the sets $\mathcal{N}_i$ in Lemma VI.2 can be taken in the form $\mathcal{N}_i := \{(x, \mathbf{0}_k) \in \mathbb{R}^{2k} : \|x - x_f\| < \nu_i\}$ for some $\nu_i > 0$ and if RANDOM_STATE samples uniformly points of the form $(x_f, \mathbf{0}_k) \in \mathbb{R}^{2k}$, then (i) in Proposition VI.4 holds. Furthermore, FIND_CLF can return the explicit expression of the CLF used in Proposition IV.10. We note also that Assumption (iii) is not restrictive, and Assumption (iv) holds by taking the parameter η sufficiently large. ●

Remark VI.6. *(Computational Complexity of C-CLF-CBF-RRT):* The computational complexity of C-CLF-CBF-RRT is the same as GEOM-RRT except for the added complexity of the COMPATIBILITY function. In general, the optimization problems (6), (7), and (23) required by COMPATIBILITY can be non-convex, which makes them not computationally tractable. However, in the setting considered in Proposition IV.6, the worst-case complexity of COMPATIBILITY is that of solving τ QCQPs, for which efficient heuristics exist [38]. In the setting considered in Proposition IV.7, (6), (7), and (23) can be solved in closed form, which means that C-CLF-CBF-RRT has the same computational complexity as GEOM-RRT. ●

Remark VI.7. *(Controller Execution):* Given a CLF-CBF compatible path $\mathcal{A}$, executing the controller (21) has the agent converge from one waypoint to the next asymptotically. However, under the assumptions of Proposition VI.4, there exist neighborhoods around the waypoints of $\mathcal{A}$ such that any two points of two consecutive neighborhoods can be connected with a CLF-CBF controller (possibly, with adjusted CLF, and

extended class $\mathcal{K}_\infty$ functions, cf. Lemma VI.2). Therefore, by executing the controller (21) for a sufficiently large but finite time, the agent can visit these different neighborhoods and trace a path whose waypoints are close to those of $\mathcal{A}$. ∎

Remark VI.8. (*C-CLF-CBF-RRT for Higher-Relative Degree Systems*): C-CLF-CBF-RRT can be adapted to the setting where h is a HOCBF, cf. Section IV-D, with the following modifications:

   (i) x_{init} and $\mathcal{X}_{\text{goal}}$ lie in $\mathcal{C} \cap \mathcal{C}_2 \cap \ldots \cap \mathcal{C}_m$;
   (ii) RANDOM_STATE returns states from $\mathcal{C} \cap \mathcal{C}_2 \cap \ldots \cap \mathcal{C}_m$ (or a subset of it consisting of stabilizable points);
   (iii) COMPATIBILITY employs the conditions described in Proposition IV.9 instead of those in Proposition IV.1 to check the compatibility of CLFs and HOCBFs. ∎

VII. SIMULATION AND EXPERIMENTAL VALIDATION

Here we illustrate the performance of C-CLF-CBF-RRT in simulation and hardware experiments. Throughout the section, we deal with a differential-drive robot following the unicycle dynamics:

$$\dot{x} = v\cos(\theta), \tag{26a}$$
$$\dot{y} = v\sin(\theta), \tag{26b}$$
$$\dot{\theta} = \omega, \tag{26c}$$

where $s = [x, y] \in \mathbb{R}^2$ is the position of the robot, θ its heading, and v and ω are its linear and angular velocity control inputs, respectively. Following [42, Section IV], we set

$$R(\theta) = \begin{bmatrix} \cos\theta & -\sin\theta \\ \sin\theta & \cos\theta \end{bmatrix}, \quad p = \begin{bmatrix} x \\ y \end{bmatrix} + lR(\theta)e_1,$$

where $e_1 = [1,0]^T$ and $l > 0$ is a design parameter. This defines p as a point orthogonal to the wheel axis of the robot. Moreover, let

$$L = \begin{bmatrix} 1 & 0 \\ 0 & 1/l \end{bmatrix}.$$

Even though the dynamics (26) are nonlinear, it follows that $\dot{p} = R(\theta)L^{-1}u$, where $u = [v, w]^T$. By defining the new control input $\tilde{u} = R(\theta)L^{-1}u$, the state p follows single integrator dynamics. The original angular and linear velocity inputs can be easily obtained from $\tilde{u}$ as $u = LR(\theta)^{-1}\tilde{u}$. Since p can be made arbitrarily close to $[x,y]$ by taking l sufficiently small, in what follows we consider p as our state variable.

A. Computer Simulations

We have tested C-CLF-CBF-RRT in different simulation environments in a high-fidelity Unity simulator on an Ubuntu PC with Intel Core i9-13900K 3 GHz 24-Core processor. We utilize the function minimize from the library SCIPY [47] to solve the optimization problems in the COMPATIBILITY function. The robots used in the simulation are Clearpath Husky[1] robots, which have the same LIDAR and sensor capabilities as the real ones, and these are used to run a SLAM system that allows each robot to localize itself in the environment and obtain its current state, which is needed to implement

[1]Spec. sheets for the Husky and Jackal robots can be found at https://clearpathrobotics.com

the controller from (21). The first simulation environment consists of a series of red obstacles whose projection on the navigation plane is either a circle or a polytope. The second simulation consists of an environment with different rooms. The different walls are modelled as obstacles using nonsmooth CBFs, given that their projection on the navigation plane are quadrilaterals. To ensure that the whole physical body of the robot remains safe, we add a slack term to the CBF that takes into account the robot dimensions. For example, for a circular obstacle with center at $x_c \in \mathbb{R}^2$ and radius $r > 0$, and a circular robot with radius $r_0 > 0$, the CBF can be taken as $h(x) = \|x - x_c\|^2 - (r + r_0)^2$. Both simulation environments have dimensions $20m \times 50m$, and in each of them the projection of the obstacles in the navigation plane is either a circle or a polytope, so the COMPATIBILITY function runs efficiently (cf. Section IV). Figure 2 shows the tree generated by C-CLF-CBF-RRT in both simulation experiments, as well as the corresponding trajectory executed by the robot using the controller obtained as the solution of (21), which successfully reaches the end goal while remaining collision-free. In both simulation environments, we use $\alpha_l(s) = 5s$ for all $l \in [M]$ and $\eta = 2m$. Once the robot is within $0.5m$ of a given waypoint, we switch the controller so that it steers the robot towards the next waypoint.

B. Hardware Experiments

We have also tested C-CLF-CBF-RRT in a physical environment using a Clearpath Jackal robot. The robot is equipped with GPS, IMU and LIDAR sensors, which are used to run a SLAM system to localize its position in the environment and execute the controller from (21). The environment, with dimensions $4m \times 9m$, consists of different obstacles whose projection on the navigation plane is either a circle or a polytope. We ensure the whole physical body of the robot remains safe using a slack term in the CBF formulation, as described in Section VII-A. Figure 3(a) shows the tree generated by C-CLF-CBF-RRT as well as the trajectory executed by the robot, successfully reaching its goal. We use $\alpha_l(s) = 5s$ for all $l \in [M]$ and choose $\eta = 2m$. Once the robot is within $0.5m$ of a given waypoint, we switch the controller so that it steers the robot towards the next waypoint.

C. Comparison with GEOM-RRT

Here we compare the performance of C-CLF-CBF-RRT with GEOM-RRT in both the simulation and hardware environments. Figure 3(b) shows the tree generated by GEOM-RRT as well as the trajectory executed by the robot in the hardware environment using the controller obtained from (21). One can observe that the trajectory generated by the robot is unable to reach the end goal and stops rather early, at a point where the optimization problem (21) becomes infeasible. This occurs because GEOM-RRT does not take into account the dynamic feasibility of the path it generates.

We should point out that the steering parameter η critically affects the performance of GEOM-RRT. To show this, we run various executions of GEOM-RRT in the simulation environment with obstacles depicted in Figure 2(a). Table I shows that smaller values of η yield a higher percentage of feasible paths
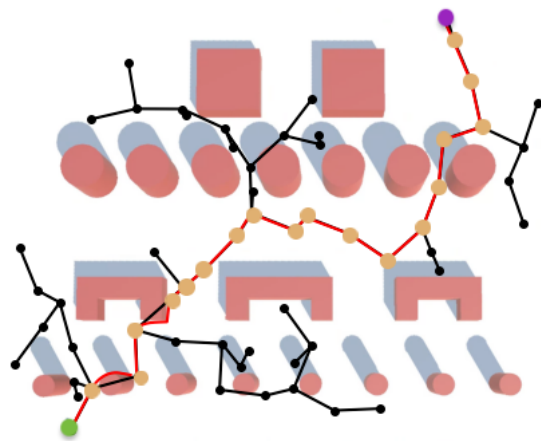
(a) Environment with obstacles
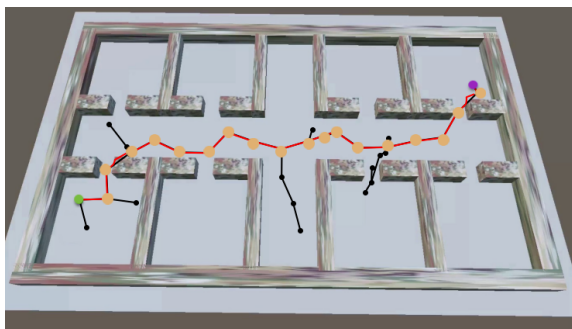
(b) Environment with rooms

Fig. 2: (a) First and (b) second simulation environment experiments. Tree generated by `C-CLF-CBF-RRT` (black), waypoints of the returned path (dark yellow) and trajectory followed by the robot using the controller from (21) (red). The starting point is the green dot and the end goal is the purple dot. In each environment, the robot successfully visits the waypoints while avoiding collisions with obstacles.

but with a higher average execution time. For comparison, the average execution time of `C-CLF-CBF-RRT`, whose paths are always dynamically feasible, for the same simulation environment and with $\eta = 4m$, is 8.72 seconds. To match the dynamic feasibility of the produced paths, `GEOM-RRT` has to be run with $\eta = 1m$, at a significantly higher computational cost.

| η (meters)	Percentage of feasible paths	Average execution time (seconds)
1	100%	154.36
2	90%	140.62
4	50%	130.62
8	30%	4.83
16	5%	1.84

TABLE I: Comparison of the percentage of feasible paths (i.e., paths for which the controller in (5) steers the robot from the initial point to the end goal by following the waypoints generated by the path) and the average execution time of `GEOM-RRT` (over 20 executions). The paths are generated for the simulation environment with obstacles in Figure 2(a).

D. Comparison with `CBF-RRT`

Here we compare `C-CLF-CBF-RRT` with `CBF-RRT`, a sampling-based motion planning algorithm proposed in [30]

(a) `C-CLF-CBF-RRT`
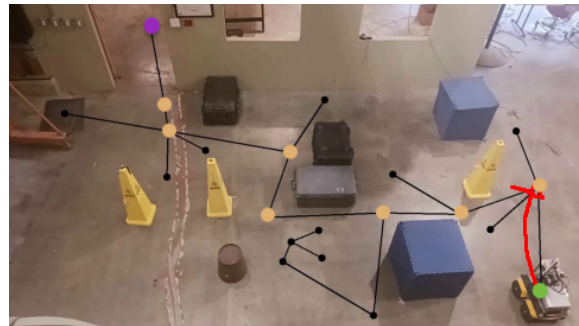
(b) `GEOM-RRT`

Fig. 3: Execution of (a) `C-CLF-CBF-RRT` and (b) `GEOM-RRT` in the hardware experiment. In both plots, tree generated by the corresponding algorithm (black), waypoints of the returned path (dark yellow), and trajectory followed by the robot (red) using the controller from (21) (red). The starting point is the green dot and the end goal is the purple dot. The trajectory executed by the robot under `C-CLF-CBF-RRT` reaches its goal safely, whereas it fails under `GEOM-RRT` because it quickly encounters a point where the optimization problem (21) is infeasible.

that also employs control barrier functions. Initially, `CBF-RRT` starts with a tree consisting of a single node in x_{init}. Then, each iteration of `CBF-RRT` operates as follows. First, it randomly samples a vertex x_0 from the current tree. Next, it generates a reference input, e.g., one steering the robot from x_0 to the goal set $\mathcal{X}_{\text{goal}}$ (cf. [30, Section 5] for more details). Finally, for a fixed period of time T_0, at every state it executes the controller closest to the reference input that satisfies the CBF condition. The state x_{new} reached by the robot after this period of time T_0 gets added to the tree.

We have ran multiple times `C-CLF-CBF-RRT` and `CBF-RRT` in the simulation environment with obstacles of Figure 2(a). Note that `CBF-RRT` is more computationally costly, as it requires running a trajectory for every new node added to the tree. Furthermore, this trajectory is generated by a controller that is obtained as the solution of an optimization problem at every point. In contrast, `C-CLF-CBF-RRT` only requires solving a single optimization problem (and, in the cases discussed in Section IV-C, not even that, since an algebraic check is enough) for every new node added to the tree. For example, if T_0 is small (e.g., $T_0 = 5$), the average execution time of `CBF-RRT` exceeds one minute. For $T_0 = 15$, the average execution time of `CBF-RRT` (over 10 different runs) is 384.58 seconds. The average execution time is similar for $T_0 = 10$, $T_0 = 20$. These numbers seem to indicate that smaller values of T_0 find a feasible path more rapidly, but such

paths contain a larger number of waypoints. In contrast, larger values of T_0 lead to paths with a smaller number of waypoints but require more time to be found. In comparison, the average execution time of `C-CLF-CBF-RRT` with the same initial point and end goal (and with $\alpha_l(s) = 5s$ for all $l \in [M]$ and $\eta = 4m$) is 8.72 seconds, almost two orders of magnitude faster.

VIII. CONCLUSIONS

We have introduced `C-CLF-CBF-RRT`, a sampling-based motion planning algorithm that generates dynamically feasible collision-free paths from an initial point to an end goal. The algorithm creates a sequence of waypoints and results in a well-defined CLF-CBF-based controller that generates trajectories guaranteed to be safe and to sequentially visit the waypoints. These guarantees are based on a result of independent interest that shows that the problem of verifying whether a CLF and a BNCBF are compatible in a set of interest can be solved by finding the optimal value of an optimization problem. For systems with linear dynamics, quadratic CLFs, and CBFs of polytopic obstacles, this optimization problem is a QCQP, and for CBFs of circular obstacles, it can be solved in closed form, ensuring the efficient execution of `C-CLF-CBF-RRT`. Finally, we have shown that `C-CLF-CBR-RRT` is probabilistically complete and can be generalized to systems where safety constraints have a high relative degree. Simulations and hardware experiments illustrate the performance and computational benefits of `C-CLF-CBR-RRT`. Future work will explore the extension of the results to other sampling-based algorithms (e.g., RRT*, bidirectional RRT), identify other classes of systems and safe sets for which the process of checking CLF-CBF compatibility can be done efficiently, and consider systems under uncertainty, both in the robot dynamics and the obstacles in the environment.

ACKNOWLEDGMENTS

REFERENCES

[1] L. E. Kavraki, P. Švestka, J. C. Latombe, and M. H. Overmars, "Probabilistic roadmaps for path planning in high-dimensional space," *IEEE Transactions on Robotics and Automation*, vol. 12, no. 4, pp. 566–580, 1996.

[2] S. M. LaValle, "Rapidly-exploring random trees : a new tool for path planning," *The Annual Research Report*, 1998.

[3] J. Kuffner and S. LaValle, "RRT-connect: an efficient approach to single-query path planning," in *IEEE Int. Conf. on Robotics and Automation*, San Francisco, USA, 2000, pp. 995–1001.

[4] S. Karaman and E. Frazzoli, "Sampling-based algorithms for optimal motion planning," *International Journal of Robotics Research*, vol. 30, no. 7, pp. 846–894, 2011.

[5] S. M. LaValle, *Planning Algorithms*. Cambridge University Press, 2006, available at http://planning.cs.uiuc.edu.

[6] D. J. Webb and J. van den Berg, "Kinodynamic RRT*: Asymptotically optimal motion planning for robots with linear dynamics," in *IEEE Int. Conf. on Robotics and Automation*, Karlsruhe, Germany, 2013, pp. 5054–5061.

[7] L. Yi, Z. Littlefield, and K. E. Bekris, "Asymptotically optimal sampling-based kinodynamic planning," *International Journal of Robotics Research*, vol. 35, no. 5, pp. 528–564, 2016.

[8] E. Glassman and R. Tedrake, "A quadratic regulator-based heuristic for rapidly exploring state space," in *IEEE Int. Conf. on Robotics and Automation*, Anchorage, USA, 2010, pp. 5021–5028.

[9] A. Perez, R. Platt, G. Konidaris, L. Kaelbling, and T. Lozano-Perez, "Optimal sampling-based motion planning with automatically derived extension heuristics," in *IEEE Int. Conf. on Robotics and Automation*, St. Paul, USA, 2012, pp. 2537–2542.

[10] A. J. LaValle, B. Sakcak, and S. M. LaValle, "Bang-bang boosting of RRTs," in *IEEE/RSJ Int. Conf. on Intelligent Robots & Systems*, Detroit, USA, 2023, pp. 2869–2876.

[11] L. Palmieri and K. O. Arras, "Distance metric learning for RRT-based motion planning with constant-time inference," in *IEEE Int. Conf. on Robotics and Automation*, Seattle, USA, 2015, pp. 637–643.

[12] Y. Li and K. E. Bekris, "Learning approximate cost-to-go metrics to improve sampling-based motion planning," in *IEEE Int. Conf. on Robotics and Automation*, Shanghai, China, 2011, pp. 4196–4201.

[13] W. J. Wolfslag, M. Bharatheesha, T. M. Moerland, and M. Wisse, "RRT-CoLearn: Towards kinodynamic planning without numerical trajectory optimization," *IEEE Robotics and Automation Letters*, vol. 3, no. 3, pp. 1655–1662, 2018.

[14] H. L. Chiang, J. Hsu, M. Fiser, L. Rapia, and A. Faust, "RL-RRT: kinodynamic motion planning via learning reachability estimators from RL policies," *IEEE Robotics and Automation Letters*, vol. 4, no. 4, pp. 4298–4305, 2019.

[15] Z. Artstein, "Stabilization with relaxed controls," *Nonlinear Analysis*, vol. 7, no. 11, pp. 1163–1173, 1983.

[16] A. D. Ames, S. Coogan, M. Egerstedt, G. Notomista, K. Sreenath, and P. Tabuada, "Control barrier functions: theory and applications," in *European Control Conference*, Naples, Italy, 2019, pp. 3420–3431.

[17] P. Wieland and F. Allgöwer, "Constructive safety using control barrier functions," *IFAC Proceedings Volumes*, vol. 40, no. 12, pp. 462–467, 2007.

[18] A. D. Ames, X. Xu, J. W. Grizzle, and P. Tabuada, "Control barrier function based quadratic programs for safety critical systems," *IEEE Transactions on Automatic Control*, vol. 62, no. 8, pp. 3861–3876, 2017.

[19] L. Wang, A. Ames, and M. Egerstedt, "Safety barrier certificates for collisions-free multirobot systems," *IEEE Transactions on Robotics*, vol. 33, no. 3, pp. 661–674, 2017.

[20] P. Mestres and J. Cortés, "Optimization-based safe stabilizing feedback with guaranteed region of attraction," *IEEE Control Systems Letters*, vol. 7, pp. 367–372, 2023.

[21] A. D. Ames, J. W. Grizzle, and P. Tabuada, "Control barrier functions based quadratic programming with application to adaptive cruise control," in *IEEE Conf. on Decision and Control*, 2014, pp. 6271–6278.

[22] S. Hsu, X. Xu, and A. D. Ames, "Control barrier function based quadratic programs with applications to bipedal robot walking," in *American Control Conference*, Chicago, USA, July 2015.

[23] M. F. Reis, A. P. Aguilar, and P. Tabuada, "Control barrier function-based quadratic programs introduce undesirable asymptotically stable equilibria," *IEEE Control Systems Letters*, vol. 5, no. 2, pp. 731–736, 2021.

[24] X. Tan and D. V. Dimarogonas, "On the undesired equilibria induced by control barrier function based quadratic programs," *Automatica*, vol. 159, p. 111359, 2024.

[25] Y. Chen, P. Mestres, E. Dall'Anese, and J. Cortés, "Characterization of the dynamical properties of safety filters for linear planar systems," in *IEEE Conf. on Decision and Control*, Milan, Italy, 2024, to appear.

[26] W. S. Cortez and D. V. Dimarogonas, "On compatibility and region of attraction for safe, stabilizing control laws," *IEEE Transactions on Automatic Control*, vol. 67, no. 9, pp. 7706–7712, 2022.

[27] P. Ong and J. Cortés, "Universal formula for smooth safe stabilization," in *IEEE Conf. on Decision and Control*, Nice, France, Dec. 2019, pp. 2373–2378.

[28] A. Ahmad, C. Belta, and R. Tron, "Adaptive sampling-based motion planning with control barrier functions," in *IEEE Conf. on Decision and Control*, Cancun, Mexico, Dec. 2022, pp. 4513–4518.

[29] K. Majd, S. Yaghoubi, T. Yamaguchi, B. Hoxha, D. Prokhorov, and G. Fainekos, "Safe navigation in human occupied environments using sampling and control barrier functions," in *IEEE/RSJ Int. Conf. on Intelligent Robots & Systems*, Prague, Czech Republic, 2021, pp. 5794–5800.

[30] G. Yan, B. Vang, Z. Serlin, C. Belta, and R. Tron, "Sampling-based motion planning using control barrier functions," in *International Conference on Automation, Control and Robots*, Prague, Czech Republic, 2019, pp. 22–29.

[31] A. Manjunath and Q. Nguyen, "Safe and Robust Motion Planning for Dynamic Robotics via Control Barrier Functions," in *IEEE Conf. on Decision and Control*, Austin, USA, 2021, pp. 2122–2128.

[32] E. D. Sontag, *Mathematical Control Theory: Deterministic Finite Dimensional Systems*, 2nd ed., ser. TAM. Springer, 1998, vol. 6.

[33] R. A. Freeman and P. V. Kototovic, *Robust Nonlinear Control Design: State-space and Lyapunov Techniques*. Cambridge, MA, USA: Birkhauser Boston Inc., 1996.

[34] P. Glotfelter, J. Cortés, and M. Egerstedt, "Nonsmooth approach to controller synthesis for Boolean specifications," *IEEE Transactions on Automatic Control*, vol. 66, no. 11, pp. 5160–5174, 2021.

[35] M. Kleinbort, K. Solovey, Z. Littlefield, K. Bekris, and D. Halperin, "Probabilistic completeness of RRT for geometric and kinodynamic planning with forward propagation," *IEEE Robotics and Automation Letters*, vol. 4, no. 2, pp. i–vii, 2019.

[36] R. T. Rockafellar, *Convex Analysis*. Princeton University Press, 1970.

[37] P. Mestres, A. Allibhoy, and J. Cortés, "Regularity properties of optimization-based controllers," *European Journal of Control*, 2024, to appear.

[38] J. Park and S. Boyd, "General heuristics for nonconvex quadratically constrained quadratic programming," *arXiv preprint arXiv:1703.07870v2*, 2017.

[39] W. Xiao and C. Belta, "Control barrier functions for systems with high relative degree," in *IEEE Conf. on Decision and Control*, Nice, France, Dec. 2019, pp. 474–479.

[40] H. K. Khalil, *Nonlinear Systems*, 3rd ed. Prentice Hall, 2002.

[41] G. Yang, C. Belta, and R. Tron, "Self-triggered control for safety critical systems using control barrier functions," in *American Control Conference*, Philadelphia, USA, Jul. 2019, pp. 4454–4459.

[42] P. Glotfelter, I. Buckley, and M. Egerstedt, "Hybrid nonsmooth barrier functions with applications to provably safe and composable collision avoidance for robotic systems," *IEEE Robotics and Automation Letters*, vol. 4, no. 2, pp. 1303–1310, 2019.

[43] P. Mestres, C. Nieto-Granda, and J. Cortés, "Distributed safe navigation of multi-agent systems using control barrier function-based controllers," *IEEE Robotics and Automation Letters*, vol. 9, no. 7, pp. 6760–6767, 2024.

[44] W. Tan, "Nonlinear control analysis and synthesis using sum-of-squares programming," Ph.D. dissertation, University of California, Berkeley, 2006.

[45] Y.-C. Chang, N. Roohi, and S. Gao, "Neural Lyapunov control," in *Conference on Neural Information Processing Systems*, vol. 32, Vancouver, Canada, Dec. 2019, pp. 3240–3249.

[46] R. D. Yates and D. J. Goodman, *Probability and Stochastic Processes: A Friendly Introduction for Electrical and Computer Engineers*. John Wiley and Sons, 2004.

[47] P. Virtanen, R. Gommers, T. E. Oliphant *et al.*, "SciPy 1.0: Fundamental Algorithms for Scientific Computing in Python," *Nature Methods*, vol. 17, pp. 261–272, 2020.

APPENDIX

The following result shows that the problem of checking whether the optimization problem (22) is feasible can be simplified by including only the constraints associated with the obstacles that intersect with Θ.

Lemma A.1. *(Reduction of the set of CBFs): Let $x_{near} \in \mathbb{R}^n$ and define $\Theta = \{x \in \mathbb{R}^n : V(x) \leq V(x_{near})\}$. Let $\mathcal{L} := \{l \in [M] : \Theta \cap \mathrm{Cl}(\mathcal{O}_l) = \emptyset\}$. Suppose that there exists a set of extended class $\mathcal{K}_\infty$ functions $\{\alpha_l\}_{l\in\mathcal{L}}$ such that the problem*

$$\min_{u\in\mathbb{R}^m} \frac{1}{2}\|u\|^2 \tag{27}$$
$$s.t. \ L_f h_{j,l}(x) + L_g h_{j,l}(x)u \geq -\alpha_l(h_{j,l}(x)),$$
$$\forall j \in \mathcal{I}_l(x), l \in \mathcal{L},$$
$$L_f V(x) + L_g V(x)u + W(x) \leq 0.$$

is feasible for all $x \in \Theta \cap \mathcal{F}$ and there exists a bounded controller $\hat{u} : \Theta \cap \mathcal{F} \to \mathbb{R}^m$ satisfying the constraints in (27) for all $x \in \Theta \cap \mathcal{F}$. Then, there exists a set of extended class $\mathcal{K}_\infty$ functions $\{\alpha_l\}_{l\in[M]}$ such that (22) is feasible for all $x \in \Theta \cap \mathcal{F}$.

Proof. Note that since $\mathrm{Cl}(\mathcal{O}_l)$ is a closed set and $\Theta \cap \mathrm{Cl}(\mathcal{O}_l) = \emptyset$ for all $l \in [M]\backslash\mathcal{L}$, there exists $d > 0$ such that $h_l(x) \geq d$ for all $l \in [M]\backslash\mathcal{L}$ and $x \in \mathbb{R}^n$. Now, take $\hat{\alpha}$ such that

$$\hat{\alpha} > \frac{\sup_{x\in\Theta\cap\mathcal{F}} |L_f h_{j,l}(x) + L_g h_{j,l}(x)\hat{u}(x)|}{d}$$

for all $l \in [M]\backslash\mathcal{L}$ and $j \in \mathcal{I}_l(x)$. Note that such $\hat{\alpha}$ exists because $\hat{u}$ is bounded and Θ is compact. Now, $\hat{u}(x)$ is also feasible for (22) for any $x \in \Theta \cap \mathcal{F}$ by taking $\alpha_l(s) = \hat{\alpha}s$ for all $l \in [M]\backslash\mathcal{L}$. $\square$

Pol Mestres received the Bachelor's degree in mathematics and the Bachelor's degree in engineering physics from the Universitat Politècnica de Catalunya, Barcelona, Spain, in 2020, and the Master's degree in mechanical engineering in 2021 from the University of California, San Diego, La Jolla, CA, USA, where he is currently a Ph.D candidate. His research interests include safety-critical control, optimization-based controllers, distributed optimization and motion planning.

Carlos Nieto-Granda is a Research Scientist in the Science of Intelligent Systems Division at the U.S. Army Research Laboratory (DEVCOM/ARL). He has obtained a B.S. degree in Electronics Systems from Tecnológico de Monterrey, Campus Estado de Mexico, Mexico; an M.S. degree in Computer Science from Georgia Institute of Technology; and a Ph.D. degree in Intelligent Systems, Robotics, and Control from University of California San Diego. His research interests include autonomous exploration, coordination, and decision-making for heterogeneous multi-robot teams focused on state estimation, sensor fusion, computer vision, localization and mapping, autonomous navigation, and control in complex environments. He is a recipient of the 2022 Transactions on Robotics King-Sun Fu Memorial Best Paper Award.

Jorge Cortés (M'02, SM'06, F'14) received the Licenciatura degree in mathematics from Universidad de Zaragoza, Zaragoza, Spain, in 1997, and the Ph.D. degree in engineering mathematics from Universidad Carlos III de Madrid, Madrid, Spain, in 2001. He held postdoctoral positions with the University of Twente, Twente, The Netherlands, and the University of Illinois at Urbana-Champaign, Urbana, IL, USA. He was an Assistant Professor with the Department of Applied Mathematics and Statistics, University of California, Santa Cruz, CA, USA, from 2004 to 2007. He is a Professor and Cymer Corporation Endowed Chair in High Performance Dynamic Systems Modeling and Control at the Department of Mechanical and Aerospace Engineering, University of California, San Diego, CA, USA. He is a Fellow of IEEE, SIAM, and IFAC. His research interests include distributed control and optimization, network science, nonsmooth analysis, reasoning and decision making under uncertainty, network neuroscience, and multi-agent coordination in robotic, power, and transportation networks.